DEPARTMENT OF ELECTRICAL
AND COMPUTER ENGINEERING

BEATRIZ MARIA RODRIGUES REIS
Licenciada em Ciências da Engenharia

DISSERTATION REPORT

LEO SIGNALS DESIGN AND DEFINITION: EXPERIMENTAL SETUP AND TRADE-OFF CONSIDERATIONS

MASTER IN ELECTRICAL AND COMPUTER ENGINEERING

NOVA University Lisbon
November, 2024

DEPARTMENT OF ELECTRICAL
AND COMPUTER ENGINEERING

DISSERTATION REPORT

LEO SIGNALS DESIGN AND DEFINITION:
EXPERIMENTAL SETUP AND TRADE-OFF CONSIDERATIONS

BEATRIZ MARIA RODRIGUES REIS

Licenciada em Ciências da Engenharia

Advisers: Pedro Boto
GNSS Engineer, GMV Innovation Solutions
Rodolfo Oliveira
Associate Professor with Habilitation, NOVA University Lisbon

Examination Committee

Chair: Luís Oliveira
Associate Professor with Habilitation, NOVA University of Lisbon

Rapporteur: Luís Bernardo
Associate Professor with Habilitation, NOVA University of Lisbon

Member: Pedro Boto
GNSS Engineer, GMV Innovating Solutions

MASTER IN ELECTRICAL AND COMPUTER ENGINEERING

NOVA University Lisbon
November, 2024

Dissertation Report

LEO signals Design and Definition: experimental setup and trade-off considerations

This document was created with the (pdf/Xe/Lua)LaTeX processor and the NOVAthesis template (v6.10.10) [**novathesis-manual**].

To my family and the incredible people I met along the way -
thank you for making this journey unforgettable.

Acknowledgements

First and foremost, I would like to express my deepest gratitude to Teresa Ferreira and Pedro Fernandes for giving me the opportunity to undertake my Thesis at GMV and for all the trust and kindness from day one. It means the world to me, and I will always be grateful for that.

To Pedro Boto, my supervisor. If someone asked me what defines a good mentor, I would say it is everything you have been to me. Thank you for always being available, for all the calm and reassurance you offered throughout this journey, and for always believing in me from the beginning. All the words of "Don't stress, you are doing great. We are on the right path", might have seemed simple, but they had a huge impact on me.

To Bárbara, my right hand, who was an essential pillar through this entire process. Thank you for always being ready to help. No matter when or how muck work you had to do, you would always find time to sit by my side and clarify all my questions. And to Inês, who often was the voice of reason and calm. To the both of you, I am really thankful for all the support and memories we have built together over these months.

To the entire GMV-NAV team. You welcomed me with open arms and created an environment where I always felt at home. Thank you for always being willing to help and for showing genuine interest in my progress.

To Professor Rodolfo Oliveira, my co-supervisor, who was an important figure through my academic journey. I am truly thankful for your guidance, teachings, and availability, which helped me a lot to get here. Thank you.

I can't forget to mention the hobby that has accompanied me in such a consistent way throughout these months: climbing. Through it, I met incredible people with whom I shared amazing experiences along the way. Quickly it became my escape and my safe space for the last months.

A special thanks to my climbing partner, who was with me on every adventure and made these months unforgettable. I will always be thankful for every moment and lightness you brought to my days. I hope life always smiles back at you.

To Pedro and Marco, because none of this would have been possible without you two. Words cannot express how grateful I am to have you in my life. University wouldn't have been the amazing journey it was if it weren't for you. It was a pleasure to swim along your side and to share the same floating device with you.

To Catarina, my "rebentinho", who always showed such understanding, even during the times I wasn't as present as I wanted to be - thank you for all the love.

To Samanta, my "guapa". You always brought so much joy and comfort to my days, even being so far away from each other. Thank you for always being there, I wish you nothing but the best that life has to offer.

Above all, I want to thank my grandmother, my father, and my mother. I know you have been through a lot, and I wasn't always the easiest person to deal with during this time. Thank you for always being there, for believing in me, and for supporting me in everything I do.

“Beatriz, que livro é este?” (Pedro Fernandes)

Abstract

The growing demand for precision, robustness, and reliability in Positioning, Navigation and Timing (PNT) services has been leading to the exploration of how Low-Earth Orbit (LEO) satellites can potentially complement the existing Global Navigation Satellite System (GNSS). Current GNSS operates mainly in Medium-Earth Orbit (MEO). However, the high altitude of these satellites - which is between 2000 km and 35786 km - leads to weaker signal strength and increased susceptibility and exposure to interference, which affects positioning accuracy.

This factor puts the robustness of GNSS at risk, especially in challenging environments such as urban areas with multipath interference and indoor scenarios.

LEO satellites, located at altitudes between 250 km and 2000 km, offer an alternative and innovative solution. Their proximity to Earth allows to receive stronger signals, providing a higher resilience, while the possibility of deploying a larger number of satellites can ensure continuous coverage, especially in areas where MEO satellites fail to reach. By integrating LEO signals with the existent GNSS constellations, the PNT performance can be enhanced, providing additional measurements, increasing system redundancy, and improving reliability in challenging environments.

This Thesis explores the design and feasibility of a LEO-PNT system, from its initial definition to the signal processing phase, in two challenging environments: indoor and multipath. Key system parameters such as the optimal number of satellites, general orbital configurations, transmitted power, modulation, and transmission frequency band will be explored to evaluate the performance of a GNSS+LEO constellation through synthetic signal generation, experimental receiver testing, and Position, Velocity, Time (PVT) solution analysis. This approach provides a comprehensive view of the benefits and future direction of the LEO constellation in complementing the current Galileo GNSS system for PNT.

Keywords: LEO satellites, PNT, GNSS, MEO satellites, Positioning, Multipath interference, Indoor positioning, PVT solution

Resumo

O aumento da necessidade de precisão, robustez e fiabilidade nos serviços de Posicionamento, Navegação e Tempo (*PNT*) tem levado à exploração da forma como os satélites de órbita baixa (*LEO*) podem potencialmente complementar o atual Sistema Global de Navegação por Satélite (*GNSS*). Atualmente, o *GNSS* opera principalmente em órbita terrestre média (*MEO*). No entanto, a elevada altitude destes satélites - entre 2000 km e 35786 km - conduz a uma fraca intensidade do sinal e a uma maior suscetibilidade e exposição a interferências, o que afeta a precisão do cálculo do posicionamento.

Este fator põe em risco a robustez do sistema *GNSS*, especialmente em ambientes difíceis como zonas urbanas com interferências multicaminho e cenários interiores.

Os satélites *LEO*, localizados a altitudes entre os 250 km e 2000 km, oferecem uma solução alternativa e promissora. A sua proximidade à Terra permite que recebam sinais mais fortes e mais resilientes, enquanto que um maior número de satélites garante uma cobertura contínua, especialmente em áreas onde os satélites *MEO* podem não conseguir chegar. Ao integrar os sinais *LEO* com as constelações *GNSS* existentes, o desempenho do *PNT* pode ser melhorado, fornecendo medições adicionais, aumento da redundância do sistema e fiabilidade do mesmo em ambientes difíceis.

Esta Tese explora o desenho e a viabilidade de um sistema *LEO-PNT*. Parâmetros chave do sistema, tais como o número ótimo de satélites, configurações gerais da órbita, potência transmitida, modulação e banda de frequência serão analisados de forma a avaliar o desempenho ao complementar o sistema atual com sinais *LEO* em céu aberto, ambientes interiores e com multicaminho.

Adicionalmente, serão desenvolvidos e analisados cenários *GNSS+LEO* através da geração de sinais sintéticos, testes de um recetor experimental e análise da solução *PVT* (Posição, Velocidade e Tempo). As vantagens de adicionar os satélites *LEO* na melhoria do desempenho de *tracking* do sinal e posicionamento, particularmente em condições difíceis, será avaliado de forma a determinar o seu papel fundamental na melhoria dos sistemas *PNT* atuais.

Palavras-chave: Satélites *LEO*, *PNT*, *GNSS*, Satélites *MEO*, Posicionamento, Interferência

Multipath, Posicionamento *Indoor*, Solução *PVT*

Contents

List of Figures **xii**

List of Tables **xiv**

Acronyms **xvi**

1 Introduction **1**
- 1.1 Motivation . . . 1
- 1.2 Goals . . . 2
- 1.3 Contributions . . . 3
- 1.4 Thesis Structure . . . 4

2 Related Work **5**
- 2.1 GNSS . . . 5
  - 2.1.1 Navigation System . . . 5
  - 2.1.2 Signals . . . 6
  - 2.1.3 Position Determination . . . 13
- 2.2 Signal Processing . . . 15
  - 2.2.1 Signal Search Acquisition . . . 16
  - 2.2.2 Signal Tracking . . . 20
- 2.3 LEO Satellite Systems . . . 24
  - 2.3.1 LEO-PNT dedicated . . . 25
  - 2.3.2 Challenges of LEO-PNT Dedicated . . . 26

3 Design and Definition of the LEO Satellites System **27**
- 3.1 Basic Link Analysis and Link Budget . . . 27
  - 3.1.1 Parameters and Components Determination . . . 27
- 3.2 Testing Phase . . . 31
  - 3.2.1 Scenario Design . . . 32
  - 3.2.2 Receiver Processing . . . 41

3.2.3 Analysis of Results and Added Value 44

4 Conclusion and Future work **65**
4.1 Conclusions 65
4.2 Future Work 66

Bibliography **67**

List of Figures

2.1 Galileo Frequency Plan [11]. 6
2.2 GNSS signal structure [15]. 7
2.3 E1 CBOC Signal Modulation [11]. 8
2.4 E6 Signal Modulation [11]. 9
2.5 E5 Signal Modulation [11]. 9
2.6 Structure of a Navigation Message (adapted from [25]). 12
2.7 Keplerian Elements. 12
2.8 Receiver with 4 satellites in view. 14
2.9 The DOP effect variation of the uncertainty region (adapted from [27]). . . . 15
2.10 GNSS Receiver Architecture and Baseband Processing Block (adapted from [32]). 16
2.11 Correlation peak from the acquisition process [33]. 17
2.12 Cross-Correlation Functions of Galileo E1C Signal in Code Domain. 18
2.13 Cross-Correlation Functions of Galileo E1C Signal in Doppler Domain. . . . 18
2.14 Correlation scheme (adapted from [34]). 19
2.15 Search Space. 20
2.16 Basic diagram for the Tracking Loops [37]. 21
2.17 Scheme of a DLL Architecture [14]. 22
2.18 ACF without the Multipath effect. 23
2.19 ACF with the Multipath effect. 23

3.1 Traces of the penalty values for S6, S7 and S8 [47]. 28
3.2 Ionosphere layer representation [49]. 30
3.3 Two-Line element set for Galileo [55]. 32
3.4 TLE Title Line. 32
3.5 TLE Line 1. 32
3.6 TLE Line 2. 33
3.7 Sequence of frames showing satellite displacement over time (every 30 seconds). 36
3.8 Tiered Codes Generation [11]. 40

3.9 Skydel output with signal configurations. 40
3.10 RINEX Example File. 41
3.11 Second Order PLL Phase Error Estimate. 43
3.12 Third Order PLL Phase Error Estimate. 43
3.13 PLL standard architecture [62]. 44
3.14 SkyPlot of MEO and LEO visible Satellites for the open sky scenario. 45
3.15 SkyPlot of MEO and LEO visible Satellites for the indoor scenario. 45
3.16 CN0 results. 46
3.17 L24 - CN0, real, and imaginary part results variation. 47
3.18 E33 - CN0, real, and imaginary part results variation. 47
3.19 L24 - Doppler shift variation. 48
3.20 Code Tracking Jitter Percentile results. 49
3.21 Code Tracking Jitter for L24. 50
3.22 Code Tracking Jitter for E33. 50
3.23 Doppler results. 51
3.24 SV Availability. 52
3.25 Horizontal Deviation and Mean and STD Deviation of Position Estimates (Full Simulation vs Last 50 seconds) for Galileo in Open Sky using Kalman Filter. 53
3.26 Horizontal Deviation and Mean and STD Deviation of Position Estimates (Full Simulation vs Last 50 seconds) for Galileo+LEO in Open Sky using Kalman Filter. 54
3.27 Detailed view on the PVT error time series for Galileo+LEO in Open Sky using Kalman Filter. 55
3.28 Horizontal Deviation and Mean and STD Deviation of Position Estimates (Full Simulation vs Last 50 seconds) for Galileo+LEO in Open Sky using LS. . . . 55
3.29 Horizontal Deviation and Mean and STD Deviation of Position Estimates (Full Simulation vs Last 50 seconds) for Galileo+LEO in Indoor using Kalman Filter. 56
3.30 CN0 results in multipath scenario. 58
3.31 Code Tracking Jitter Percentile results in multipath scenario. 59
3.32 Position Horizontal Deviation for Galileo in Multipath scenario, using Kalman Filter. 60
3.33 Position Horizontal Deviation for Galileo in Multipath scenario, using Least Squares. 61
3.34 Position Horizontal Deviation for Galileo+LEO in Multipath scenario, using Kalman Filter. 62
3.35 Position Horizontal Deviation for Galileo+LEO in Multipath scenario, using Least Squares. 62

List of Tables

2.1 Galileo Central Frequencies. 7
2.2 Galileo message types. 11
2.3 LS and KF Positioning Techniques Summary. 24
2.4 LEO, MEO and GEO - Economic Aspects. 26

3.1 Line 1 structure. 33
3.2 Line 2 structure. 33
3.3 Time series Open Sky. 37
3.4 GNSS generation parameters [11]. 38
3.5 XRC configuration parameters. 42
3.6 CN0 - Mean results. 46
3.7 Code Tracking Jitter results - Percentile 95%. 50
3.8 Positioning results for Galileo+LEO in Indoor scenario and Galileo+LEO in open sky scenario, respectively. 57
3.9 SV Availability results without and with multipath, respectively. 57
3.10 CN0 - Mean values. 59
3.11 Mean and STD Deviation of Position Estimates (Full Simulation vs Last 50 seconds) for Galileo in Multipath scenario using Kalman Filter and Least Squares. 61
3.12 Mean and STD Deviation of Position Estimates (Full Simulation vs Last 50 seconds) for Galileo+LEO in Multipath scenario using Kalman Filter and Least Squares. 63

Acronyms

ACF Auto-Correlation Function *(pp. 11, 23)*
AltBOC Alternative Binary Offset Carrier *(p. 9)*

BOC Binary Offset Carrier *(p. 10)*
BPSK Binary Phase Shift Keying *(pp. 10, 31)*

C/N0 Carrier-to-Noise Density Ratio *(p. 17)*
CBOC Composite Binary Offset Carrier *(p. 8)*
CS Commercial Service *(p. 6)*

DLL Delay-locked-loop *(p. 20)*
DOP Dilution of Precision *(p. 15)*
DSSS Direct Sequence Spread Spectrum *(p. 10)*

ECEF The Earth-Centered, Earth-Fixed *(p. 53)*
ESA European Space Agency *(p. 5)*

FLL Frequency-locked-loop *(pp. 20, 42)*

GEO Geostationary Orbit *(pp. 24, 26)*
GNSS Global Navigation Satellite System *(pp. vii, 1–6, 23–25, 37, 65, 66)*

I&D Integration & Dump *(pp. 18, 21)*
IQ In-phase and Quadrature *(p. 40)*
ITU International Telecommunications Union *(p. 6)*

LEO Low-Earth Orbit *(pp. vii, 1–4, 6, 25, 26, 30, 34–36, 38, 42, 45–48, 50–52, 54, 56–58, 60, 61, 63, 65, 66)*

LEO-PNT LEO-Position, Navigation and Timing *(p. 24)*
LOS Line of Sight *(pp. 22, 26)*

MA Multiple Access *(p. 9)*
MEO Medium-Earth Orbit *(pp. vii, 1, 3, 5, 6, 13, 24, 26, 30, 34, 36, 38, 42, 47, 50, 54, 58, 63, 65)*

NCO Numerical Control Oscillators *(pp. 21, 44)*
NRZ Non Return To Zero *(p. 10)*

PDOP Position Dilution of Precision *(pp. 24, 25)*
PLL Phase-locked-loop *(pp. 20, 42–44)*
PNT Positioning, Navigation and Timing *(pp. vii, 1–3, 25, 27, 29, 64, 65)*
PPP Precise Point Positioning *(p. 24)*
PRN Pseudorandom Noise *(pp. 7–9, 11, 21, 39)*
PVT Position, Velocity, Time *(pp. vii, 1, 3, 5, 7, 12, 14, 15, 44, 53, 54, 64–66)*

SQM Signal quality monitoring *(p. 41)*
SV Space Vehicle *(pp. 6, 13)*

TLE Two-Line Element *(p. 32)*
TTFF Time to First Fix *(pp. 7, 19)*

Chapter 1

Introduction

1.1 Motivation

To fulfill the pressing demands for enhanced precision, reliability, and robustness, LEO satellites are emerging with a significant role in PNT, given their potential to revolutionize these services, which are generally provided by the GNSS.

Relying only on a single constellation, such as Galileo's, for indoor positioning, is not feasible yet with today's technology. Currently, it is not possible to depend exclusively on Galileo for this purpose, particularly in indoor and multipath environments. In such scenarios, the number of Galileo satellites with meaningful measurements will likely be less than four, which is not sufficient for a robust and accurate position calculation, not guaranteeing the necessary reliability and accuracy.

The GNSS, consisting of GPS (United States), GLONASS (Russia), GALILEO (European Union), BeiDou (China), NavIC (India), and QZSS (Japan), resides mainly in MEO - between altitudes of 2000 km and 35786 km - which contributes to weaker signals and susceptibility to interference, being a potential threat to the robustness of these systems. This challenge has contributed to the emergence of out-of-domain solutions, like LEO satellites, to provide a reliable backup for PNT-dependent systems and safeguard the national critical infrastructure [1, 2].

This is where the inclusion of LEO satellites becomes critical. By integrating these satellites into the system, it is possible to achieve positioning even in very harsh environments, which marks a significant improvement over the traditional Galileo-only approaches.

It is at this point that the added value of the current study is best seen. In this work, a LEO system will be designed, aiming at increasing the availability and robustness of PNT applications that rely on GNSS. The work will not only design the system but generate and process signals according to that design, in conjunction with Galileo satellites. Additionally, in a GNSS Software Receiver, the added value of the proposed constellation will be analysed, from a PVT and tracking loop point of view. For the results analysis, two main scenarios are going to be considered, in which, it is believed, that the new constellation will provide a high added value. Those considered scenarios are in indoor and multipath environments (mimicking an urban city center), which are expected to extract meaningful results from the inclusion of the new constellations of satellites.

It is very important to ensure that the new LEO constellation will provide added value in terms of accuracy and robustness, as user applications keep on demanding higher performance from the GNSS constellation. Additionally, important conclusions will be drawn regarding the potential use of the Galileo constellation (MEO+LEO) as a single-use constellation, without being necessary to rely on other constellations. For this reason, only Galileo was considered in the current study.

This Thesis contributes to a better understanding of these satellites, and their potential when put together with GNSS, ultimately contributing to the development and improvement of the current PNT solutions.

1.2 Goals

This work aims to design and evaluate a LEO satellite system able to be used for PNT applications (LEO-PNT), in order to investigate the potential of these satellites to overcome the limitations of the current GNSS.

The objectives involve the definition of the system parameters, such as the feasible number of LEO satellites, the best orbits for visibility, the transmitted power, the modulation to be used, and the frequency band of the transmitting signals. Moreover, scenarios including GNSS+LEO will be created and their benefits evaluated in indoor and multipath environments.

System Design and Definition

The System Design consists of the definition of the following parameters:

1. LEO Constellation Design: Define the feasible number of LEO satellites and their orbital configurations, to maximize coverage for PNT applications. The final constellation will be based on Starlink's TLE data, ensuring a more realistic scenario.
2. Power and Signal Characteristics: Define the transmitted and received power, based on current values for GNSS satellites.
3. Signal Modulation: Examine various modulation schemes that can be used for transmitting signals, ensuring compatibility with the existing GNSS system.
4. Transmission Frequency: Identify the optimal frequency band for signal transmission (according to legal requirements and ensure compatibility with the existing GNSS receivers), considering the challenging environments assessed.

Scenario Generation and Analysis

After defining the system, GNSS+LEO scenarios will be generated under different environments:

1. Open Sky Scenario: Evaluate the system in an ideal environment with full satellite visibility, used as a reference scenario.
2. Indoor Scenario: Analyse the impact and added value when combining LEO signals with GNSS in environments with limited satellite visibility.
3. Multipath Scenario: Test the system's robustness in environments where the reflected signals can decrease performance.

System Performance Evaluation

Assess the key performance metrics of the combined GNSS+LEO system such as CN0, Code Tracking Jitter Percentile, Doppler, and SV Availability, comparing it with the GNSS-only reference scenario. For this purpose, synthetic signals will be generated and processed, using an experimental receiver (with implementation of new LEO signals).

Additionally, a final examination on the PVT results is made, in order to evaluate the added value of the purposed system.

1.3 Contributions

This Thesis highlights and analyses how the integration of LEO satellites, in cooperation with the existent GNSS, can increase the potential of the Galileo constellation to function as a standalone system and also to improve its overall performance. The present work aims to demonstrate how such integration can enhance the accuracy, performance, reliability, and coverage of GNSS aiming at PNT solutions.

As it will be analyzed and demonstrated later, LEO satellites can offer increased signal power and coverage, due to their proximity to Earth. This is especially useful in challenging environments, such as those explored in this Thesis - indoor and multipath - where traditional MEO satellites face limitations.

In the work performed next there are three main components under analysis:

- Signal Generation: A completely new signal was designed where a new frequency band was introduced - the S-band - and orbits were defined in order to have a reliable number of LEO satellites in the sky.
- Receiver / Signal Processing: At the receiver processing level, a new signal was implemented, based on the previous design. Modifications/implementations were necessary at the tracking level, specifically involving a new central frequency and fine-tuning to accommodate the new dynamics of such signals in LEO orbits.
- PVT engine - Current PVT engines are not yet prepared to deal with the high dynamics introduced by the LEO orbits and the increased number of pseudoranges. Therefore, the ability to retrieve a meaningful position represents a step forward towards the full definition of such new systems.

This work contributes in terms of novelty by designing and testing a LEO-PNT system, which is currently a relatively unexplored area in GNSS. The results of this Thesis bring an innovative approach, offering a new perspective on how the current positioning systems can be optimized.

1.4 Thesis Structure

This Thesis is organized in four different parts. The first chapter, the current one, contains the introduction and a first approach to the main topic of this thesis - LEO Satellites - as a Motivation. The goals to be achieved are also presented.

Chapter 2 introduces the fundamentals of satellites, GNSS, signals, bands, and modulation specifications. This content should be mastered in order to succeed on achieving the goals of this thesis.

Chapter 3 focuses on analysing the integration of LEO satellites into GNSS, assessing the impacts on the signal dynamics, tracking aspects and performance, and positioning accuracy. Initially, the constellation is designed, which includes the definition of the frequency band, modulation, and expected power values, among other parameters. Following this theoretical approach, the Testing Phase takes place, where the fine-tuning, scenarios, and signal generation are assessed. Finally, an analysis is conducted on the overall system's performance in order to analyse the added value of LEO satellites.

In Chapter 4, a conclusion is presented, followed by proposals for future work.

Chapter 2

Related Work

2.1 GNSS

This section provides a brief overview of the GNSS, focusing on the Galileo European system.

2.1.1 Navigation System

The GNSS is a constellation of satellites in several orbits that transmits signals from space that will be used by the receivers to compute a PVT solution to be further used by a wide range of applications.

Currently, GNSS consists of six constellations: GPS, Galileo, BeiDou, GLONASS, NavIC and QZSS [3]. What these constellations have in common is the need for precise timing and accuracy. However, they do mainly differ on some characteristics, such as: the number of satellites, on the Multiple Access System being used, the amount of revolutions per day, and coverage area, among others [4].

This thesis will be focused on the Galileo satellite technology given its European origin, in addition to the future LEO constellation aimed by European Space Agency (ESA). This constellation, Galileo, came to give independence to the European Satellite navigation, while still maintaining interoperability with GPS and GLONASS. It is composed out of three segments: the space segment, control segment, and user segment [5, 6].

Space Segment: Composed of Satellites in orbit, placed in a MEO constellation, transmitting signals, which contain information on the position and time. They also store and transmit the navigation message, sent previously by the control segment, and are equipped with atomic clocks in order to guarantee a high precision.

Control / Ground Segment: This segment is responsible for sending and updating the navigation message, to calculate the Ephemeris data. It is constituted by the monitoring stations and plays a crucial role in providing corrections to achieve high precision and robustness to the system.

User Segment: Consists of the receivers and users. It receives the signals sent by the Space Segment and is able to determine the pseudoranges and calculate the position, velocity, and time as it will be later detailed.

Galileo satellites, by transmitting signals, are supporting several services, as described below [7–9]:

Open Service (OS): Free access to the users to position, navigation, and time services globally.

High Accuracy Service (HAS): Known before as Commercial Service (CS), this service provides additional accuracy on the navigation signal in a different frequency band.

Public Regulated Service (PRS): Only accessed by government-authorized users, it provides a higher level of security.

Support to Search and Rescue service (SAR): To allow real-time distress alerts with a high level of precision location.

This constellation has 30 satellites located in MEO, and to better understand its signals it is important to study how the PVT solution is computed taking into account the broadcast ranging signals that will be used in the user segment to compute a pseudorange, ρ_i, – the distance between the Space Vehicle (SV) and the receiver.

2.1.2 Signals

This section provides a detailed analysis of GNSS signals, which is important to explore the potential of the LEO satellites.

To guarantee that all services can cooperate without interfering with each other, the International Telecommunications Union (ITU) allocated the L-band frequencies to GNSS [10].

GNSS signal frequencies are located in the radio spectrum in the L-band, where Galileo transmits signals, as represented in Figure 2.1.

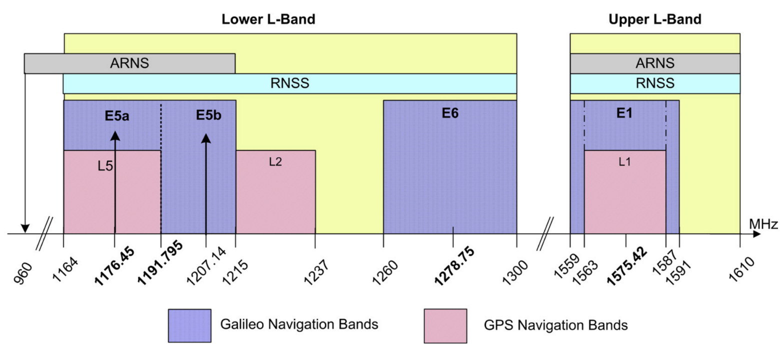

Figure 2.1: Galileo Frequency Plan [11].

Each GNSS signal is mainly composed of:

- Central Frequency: This is a radio-frequency sinusoidal component, denoted f_c. Each Galileo signal has its own central frequency, as shown in Table 2.1.

Table 2.1: Galileo Central Frequencies.

E1	E6	E5b	E5a
1575.42 MHz	1278.75 MHz	1207.14 MHz	1176.45 MHz

- Navigation Message: Denoted $d(t)$, it provides useful information on the satellite ephemeris, almanac, satellite health status, and clock information, among others. This message is only part of the GNSS data components and it allows a precise calculation of the position and navigation [12].

- Ranging-code: Each satellite is assigned a unique code, so the receiver is able to distinguish the signals from different satellites. These codes are called Pseudorandom Noise (PRN) sequences which are periodically repeated and have low cross-correlation with other signals, so satellites can transmit with low interference from each other. The ranging code is a sequence of zeros and ones, called "chips" that will allow an accurate calculation of the pseudorange and in turn the final position [13].

The main goal for a GNSS receiver is to calculate the user position and reduce the Time to First Fix (TTFF), which is the time required to acquire the PVT by processing the satellite signal retrieving the navigation data, and estimating the pseudorange [8, 14].

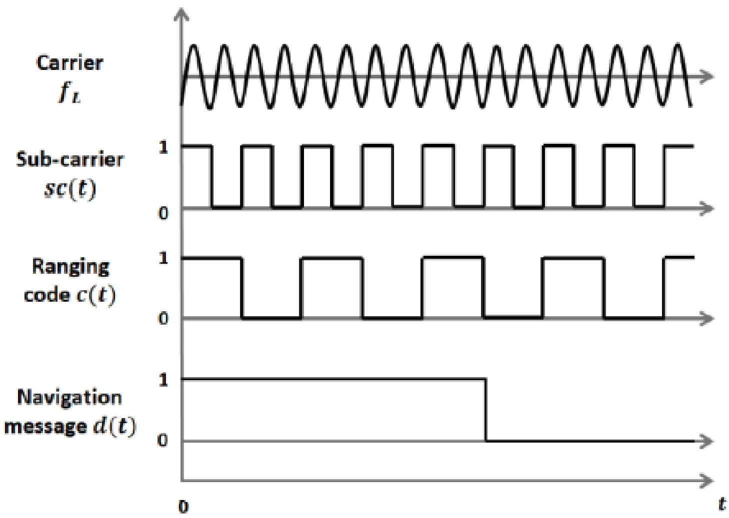

Figure 2.2: GNSS signal structure [15].

As illustrated in the signal structure diagram in Figure 2.2, the carrier, the sub-carrier, the ranging code and the Navigation message, all together, form a complex waveform.

The signal received from a satellite is represented by

$$s(t) = AD(t-\tau)c(t-\tau)\cos\left(2\pi\left(f_c + f_d\right)t + \theta\right), \tag{2.1}$$

where A is the signal amplitude, τ is the code delay from the satellite to the receiver, $D()$ is the data or message bit, $c()$ is the PRN code, f_c is the central frequency, f_d the Doppler frequency and θ the carrier phase [16].

2.1.2.1 Bands and Modulations

As shown previously in Figure 2.1, Galileo signals are transmitted in three different frequency bands: E1, E5, and E6. These configurations allow for a broader spectrum of bandwidth, increasing signal availability and spectral diversity.

E1: The E1-OS signal is characterized by a Composite Binary Offset Carrier (CBOC) modulation - CBOC(6,1,1/11) -, which is a combination (multiplexing) of BOC(1,1) and BOC(6,1) modulations in such a way that 1/11 of the power is allocated to the high frequency component [17]. This signal is divided into two components: a data component (represented by e_{E1-B}), containing the I/NAV message (D_{E1-B}) and the PRN sequence ranging code (C_{E1-B}), and a pilot component (e_{E1-C}), which is a free data channel. The BOC(1,1) modulation is represented by the sub-carriers $sc_{E1-B,a}$ and $sc_{E1-C,a}$, while the BOC(6,1) are $sc_{E1-B,b}$ and $sc_{E1-C,b}$ [18].

Figure 2.3 represents the scheme of E1 CBOC Signal Modulation. More information on the BOC modulation can be found further in this section.

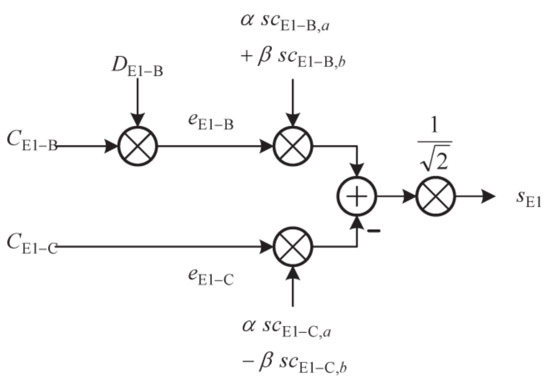

Figure 2.3: E1 CBOC Signal Modulation [11].

E6: The E6 signal has a BPSK(5) modulation and is also characterized by two components: a data component, e_{E6-B}, containing the C/NAV message (D_{E6-B}) modulated with an encrypted ranging code (C_{E6-B}), and a pilot component e_{E6-C}, which is a free of data channel. Sub-carriers are not used to modulate the ranging codes in this signal [12]. The E6 Signal Modulation is represented in Figure 2.4.

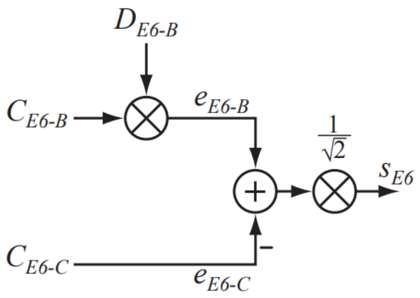

Figure 2.4: E6 Signal Modulation [11].

E5: This signal is allocated in two frequency bands: E5a and E5b. Those signals modulate E5 using the Alternative Binary Offset Carrier (AltBOC) modulation and its representation can be found in Figure 2.5.
This signal has four components: two data components and two pilot components. For the E5a signal, there is the e_{E5a-I} component from the F/NAV data (D_{E5a-I}) and for the E5b there is the e_{E5b-I} from the I/NAV data stream. Both components are modulated with the unencrypted ranging code C_{E5a-Q} and C_{E5b-Q}, respectively.

Moreover, those components are multiplexed using the AltBOC modulation [12].

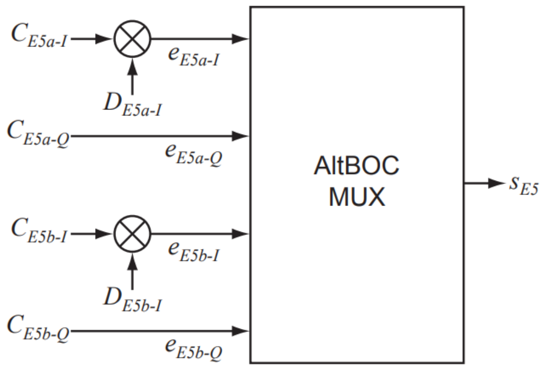

Figure 2.5: E5 Signal Modulation [11].

More information on the modulation schemes can be found in [11].

GNSS uses Spread Spectrum techniques, in which the spreading and dispreading operations are made through a PRN code attached to a communication channel (the signal is multiplied by the PRN sequence) [19]. These techniques are important due to the need of satellites to share the available bandwidth, making sure that their signals are orthogonal or separated. This is achieved through Multiple Access (MA) techniques. Most GNSS's uses DS-CDMA technique, for which the signal of each satellite is distributed in the time-frequency domain allowing the separation of different channels users (since satellites are transmitting at the same time) [8].

Below we present the most common modulation techniques used in GNSS to transmit different types of information. Direct Sequence Spread Spectrum (DSSS) spreads the signal through a larger bandwidth allowing it to be transmited over a wide frequency band [20].

BPSK

Binary Phase Shift Keying (BPSK) was the first modulation to be used for Satellite Navigation. It is known for its simplicity and so it is possible to say that if a rectangular chip pulse shape is used, then it is considered a BPSK signal.

For each symbol, the carrier signal is altered by 180 degrees, and that shift represents the binary values of 0 and 1.

It can be represented as [21]

$$p_{\Pi}(t) = \frac{1}{\sqrt{T_c}} \left[U\left(t + \frac{T_c}{2}\right) - U\left(t - \frac{T_c}{2}\right) \right], \tag{2.2}$$

where U has value 0 for $t < 0$ and 1 for $t \geq 1$ [22].

BOC

Binary Offset Carrier (BOC) modulation is the most common in the Galileo constellation and its main characteristic is the fact of concentrating the power not in its central frequency but on the frequency of the sub-carriers and can be defined with two models. The first one is generated by multiplying the PRN code $c(t)$ with a sine or cosine square wave sub-carrier sc_{BOC}. The expression of sine-phased BOC signal is

$$s(t) = c(t) \cdot \text{sign}\left[\sin(2\pi f_s t)\right], \tag{2.3}$$

with

$$c(t) = \sum_k c_k h\left(t - kT_c\right), \tag{2.4}$$

where c_k represents the code sequence, f_s the sub-carrier frequency and $h(t)$ represents the Non Return To Zero (NRZ) code.

The second model is defined as follows

$$s(t) = \sum_k c_k p_{T_c}\left(t - kT_c\right), \tag{2.5}$$

where p_{T_c} represents the chip waveform with n rectangular pulses of T_c/n duration.

BOC signals are commonly represented as $BOC(f_s, f_c)$, where $f_s = m \cdot 1.023$ (no matter what model is chosen) [8, 23].

One important parameter to be analysed is Φ, which represents the number of half periods that can fit in a chip, represented by

$$\Phi = 2\frac{f_s}{f_c}. \tag{2.6}$$

It is possible to conclude that its value can be odd or even. For odd values, some modifications have to be applied to the second model due to possible misalignment when the sub-carrier doesn't fit perfectly within the chip (polarity inversion) [22].

The updated definition for the second model is presented as [8, 23]

$$s(t) = \sum_k (-1)^k c_k p_{T_c}(t - kT_c)\,. \tag{2.7}$$

2.1.2.2 Codes and PRN sequences

As illustrated in Figure 2.2, the GNSS signal structure has a ranging code, or a PRN sequence of zeros and ones - "chips", in which

$$a = (a_0, a_1, \ldots, a_{k-1}) \text{ is a sequence of } k \text{ "chips," where } a_i \in \{-1, 1\}. \tag{2.8}$$

That sequence is unique for each satellite and has a low-cross correlation with other signals, which allows to accurately differentiate signals from different satellites. This spreading codes can be generated through an algorithm or, as in case of Galileo E1 OS, the signals use memory codes. In this case, there's no code generator algorithm and the codes need to be stored in memory [13].

The PRN codes are used due to their Auto-Correlation Function (ACF) properties that will allow to obtain a single high peak when two codes are aligned, which will contribute to good tracking results and to make the tracking process possible [24].

This means that when the code is aligned with the local replica, the correlation output is maximum. On the other hand, when the code is aligned with a non-aligned replica of itself or with another code of the same family, the correlation output will be low, which is a bad indicator. This behaviour can be analysed in Figure 2.11.

All the tracking process is done through correlations, where the output has a maximum value when there's alignment between the code and the local replica. This correlation tracking methodology is explored in detail in subsection 2.2.1.

2.1.2.3 Navigation Message and Orbits

Different types of navigation messages are broadcasted depending on the channel and service being used. Those types are illustrated on the following table 2.2.

Table 2.2: Galileo message types.

Message Type	Channel	Service
I/NAV	E1-B, E5b-I	OS/CS
F/NAV	E5a-I	OS
C/NAV	E6-B	CS

The structure of a navigation message is organized in a sequence of frames. A frame comprises multiple sub-frames, which consists of several pages. Each page has the fundamental structure that contains the navigation data [25]. An illustration of the structure can be seen in Figure 2.6.

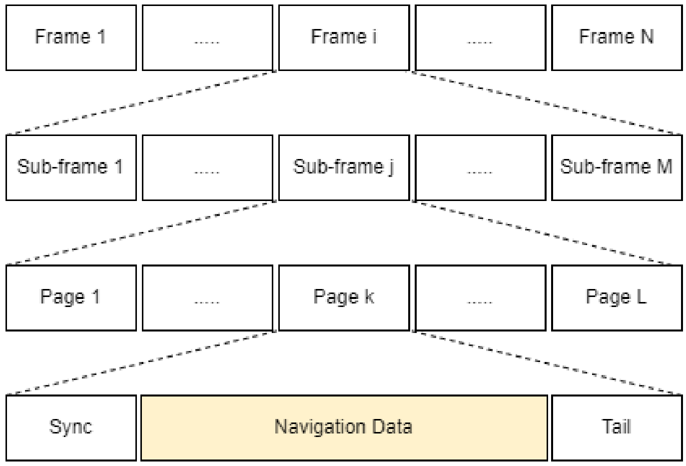

Figure 2.6: Structure of a Navigation Message (adapted from [25]).

The content of the navigation messages (specifically the navigation data) is crucial, since it is the key source of information necessary to calculate the PVT solution.

To obtain positioning different types of data are needed, and those parameters are obtained through the tracking and data demodulation process [26, 27]:

- **Ephemeris parameters** (Keplerian Orbital elements): there are six Keplerian parameters which are used to identify a specific orbit and they contain information on the satellite's location (see Figures 2.7a and 2.7b).
- **Time and Clock Correction parameters**: used for the pseudorange calculation.
- **Service Parameters**: contains the satellite ID, information on the Signal health status and a set of navigation data.
- **Almanac**: contains information on the position of all satellites in the constellation.

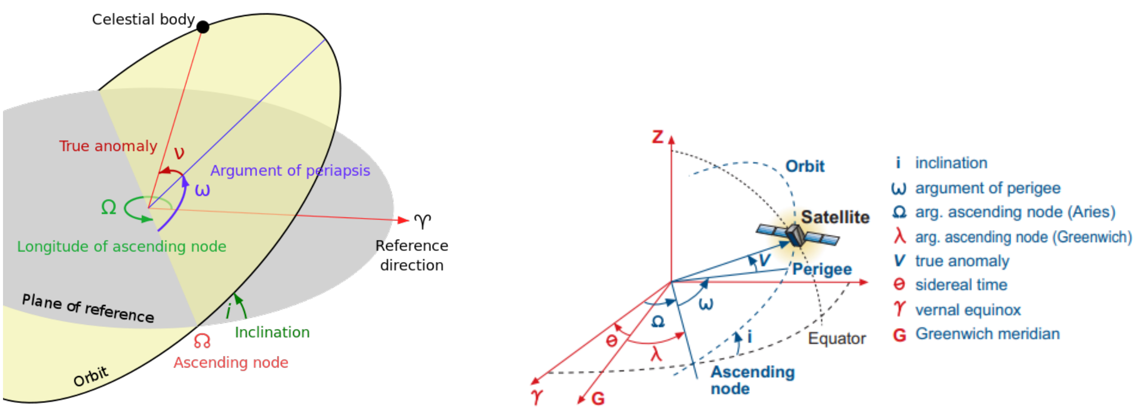

(a) Keplerian Paramters [26]. (b) Orbital Parameters [27].

Figure 2.7: Keplerian Elements.

Specific orbits are identified by six orbital parameters (see Figures 2.7(a) and 2.7(b)) [26, 27]:

- e, the *eccentricity*, is what characterizes the ellipse's shape ($e = 0$ for circular orbit, $e < 1$ for elliptical orbit, $e > 1$ for for hyperbolic trajectory and $e = 1$ for parabolic trajectory). Galileo orbits are near circular since its range values are 0.0001 to 0.0006.
- a, the *semi-major axis*, is the sum of the periapsis and apoapsis divided by two.
- i, the *inclination*, is the vertical tilt of the ellipse to the reference/equatorial plane and it is measured at the ascending node.
- Ω, the *longitude of the ascending node*, orients the ascending node of the ellipse horizontally with respect to the reference plane's vernal point γ. It is measured in a counterclockwise direction when viewed for the positive Z-axis.
- ω, the *argument of periapsis*, is the angle from the ascending node to the periapsis (which is the closest point from the satellite to the central body), defining the orientation of the ellipse.
- *Mean anomaly*, is the position of the satellite on the ellipse at a precise epoch. Can be converted to ν, which is the angle from the periapsis to the satellite.

The Galileo constellation / Space Segment (defined as 24/3/1 Walker constellation) is formed out of 30 MEO satellites, of which 6 are spare (to replace any failed satellite) and it has an orbital inclination of 56 degrees [28].

The number of visible Galileo satellites is 6 or 7, being 4 or more visible in 90% of the time [29, 30].

2.1.3 Position Determination

Galileo has in its constellation 30 satellites located in MEO, and to better understand its signals it is important to study on how the PVT solution is computed.

Those satellites broadcast ranging signals which will be used in the ground segment to compute a pseudorange, ρ_i, – distance between the SV and the receiver, represented by

$$\rho_i = c(T_r - T_i) = c\Delta T_i. \tag{2.9}$$

Then, to compute the receiver's position the following equation is used

$$\rho_i = \sqrt{(x_i - x)^2 + (y_i - y)^2 + (z_i - z)^2} + c\epsilon t_i, \tag{2.10}$$

where (x_i, y_i, z_i) are the known satellite coordinates, (x, y, z) are the unknown receiver coordinates and $c\epsilon t_i$ is the speed of light multiplied by an error due to the not synchronized clocks of the satellite and the receiver.

To solve (2.10), we need a 4 equation system, one for each satellite. This means that the user will need at least 4 pseudoranges at the same time to compute the PVT solution, as illustrated in Figure 2.8.

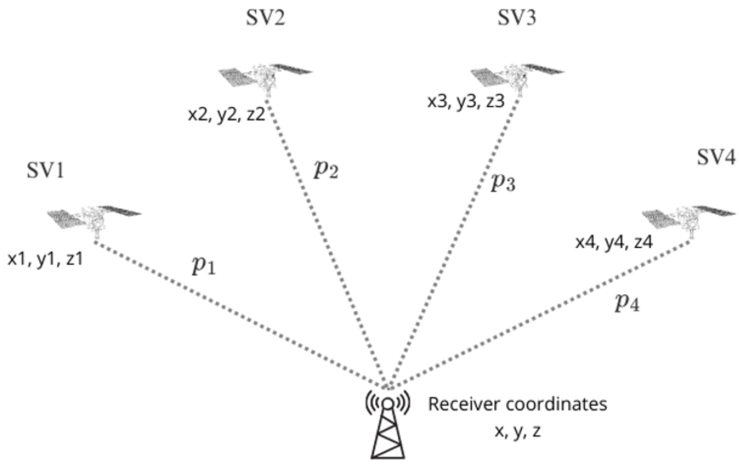

Figure 2.8: Receiver with 4 satellites in view.

The PRN code is continuously repeated every few milliseconds, and on top of it, the navigation data is also modulated, containing information on the orbit, clock, and other essential parameters.

The main goal for the receiver in the GNSS is to calculate the time for signals to travel from the satellite to the receiver. This involves generating a local copy of the PRN sequence that is continuously compared and aligned with the received signal, until the maximum correlation is obtained. This process is refered to as the "tracking loop".

Once the total transmission time is determined, it can be multiplied by the speed of light to obtain the range from the satellite to the receiver.

The GNSS signals offer three essential measurements, which will be further used to calculate the PVT solution [8, 31]:

- Pseudorange: measures the distance between the satellite and the receiver from the travel time of the signal. This distance is not the "real" distance (which is defined as range) to the satellite since it also includes the clock bias between the satellite and the receiver and also propagation errors as for example the troposphere and ionosphere contributions.

- Carrier Phase: measurement of the apparent distance (pseudorange) between the satellite and the receiver. It is more precise than the code measurements due to the fact of being intimately related with the number of cycles of the signal between the satellite and the receiver.

- Doppler Shift: measurement of the changed received frequency caused by Doppler effect. This value will be further integrated to obtain the Phase Shift, which will be used to estimate the time delay.

In addition, it is important to mention the Clock Synchronization factor. Satellite clocks are equipped with high precision atomic oscillators to stabilize, but they can still accumulate clock offsets over time. So those offsets are continuously being estimated by the ground segment and transmitted back to users. The receiver does not need to be equipped with such high grade clocks, being usually used quartz-based clocks.

The Dilution of Precision (DOP) is a crucial metric that provides an insight on how precise is the position solution, since the geometry of satellites affect that information [27]. The effect of DOP can be seen on the figure below.

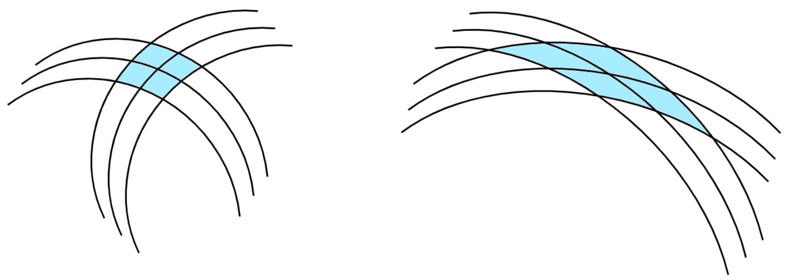

Figure 2.9: The DOP effect variation of the uncertainty region (adapted from [27]).

As can be seen on the previous figure, for two different user positions, the uncertainty region differs which will affect the final position. In the left figure, the uncertainty region is lower which in turn will provide a lower DOP that will increase the accuracy of the position.

2.2 Signal Processing

This chapter will go through the processing of a GNSS signal by a receiver, covering the key aspects of the signal search acquisition, tracking and the architecture of the receiver itself.

In the signal processing stage, the GNSS receiver is able to combine and gather all the satellite's signals, preparing them for separate analysis and digital sampling. Following this, the acquisition/tracking stage begins, where the channels synchronize, the data is decoded, and crucial satellite information, such as the Ephemeris and Almanac information, is obtained, along with the pseudorange and carrier phase estimation which are essential to calculate the PVT solution. To accomplish this, the receiver architecture plays an essential role.

GNSS receivers are designed to determine accurately the user's PVT by processing the signals from the satellites.

A general receiver, like the one represented on Figure 2.10, is composed of an analog and a digital part.

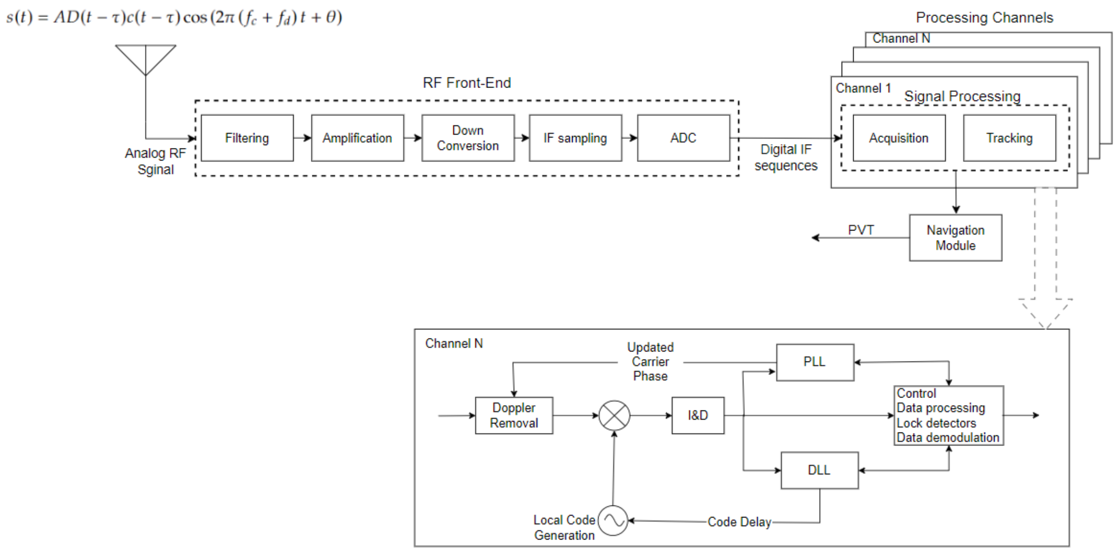

Figure 2.10: GNSS Receiver Architecture and Baseband Processing Block (adapted from [32]).

The analog part is composed of an antenna and the RF Front-End, while the digital part has the baseband processing channels, where all the signal processing happens, including the signal search acquisition and tracking loops [8]. Furthermore, in the Navigation Module, all measurements (mentioned in Subsection 2.1.3) obtained by the Processing Channels are used by the PVT engine to compute the accurate position, velocity, and time information solution.

In the next subsections, a more detailed approach to the acquisition and tracking stages is performed, to better understand how the Signal Processing stage works.

2.2.1 Signal Search Acquisition

In signal processing, the first stage that GNSS receivers go through is the acquisition, which is what allows them to detect an incoming signal, identify the visible satellites, and give a first estimation of the signal parameters.

For the receiver to be able to detect the presence of a GNSS signal, it uses the auto-correlation concept, which will be analyzed in the next section.

Correlation Concept

To better understand this current chapter, it is crucial to master the correlation concept, how it works and why it matters.

As already mentioned, the acquisition stage aims to detect the presence of a GNSS signal and estimate the code delay and the Doppler frequency, so the tracking process can start. To do so, the incoming signal is correlated with a locally generated replica of the spreading code and carrier of the signal.

The correlation operation has some GNSS signal properties, such as the spreading code properties. This means that those codes have pseudorandom characteristics, such that when the spreading code is correlated with itself, the result function equals 1, which is an indicator of a perfect alignment. When the result correlation function deviates from 1, the opposite situation happens, which means that two distinct spreading codes are correlated [13].

When a peak is generated, above a predetermined threshold of Carrier-to-Noise Density Ratio (C/N0), for example, it means that it is a good estimate. An example of a correlation peak from the acquisition process is depicted in Figure 2.11.

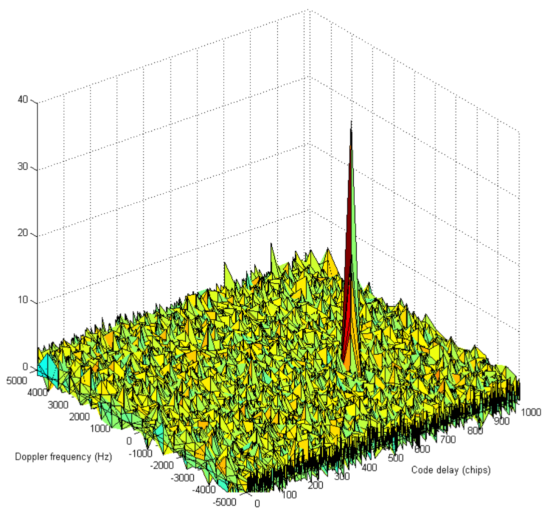

Figure 2.11: Correlation peak from the acquisition process [33].

In Figures 2.12(a), 2.12(b), 2.13(a), and 2.13(b) it is possible to analyze two-dimensions plots of the Cross-Correlation Function of a real Galileo E1C Signal in Code and Doppler domain, respectively, and identify its peaks.

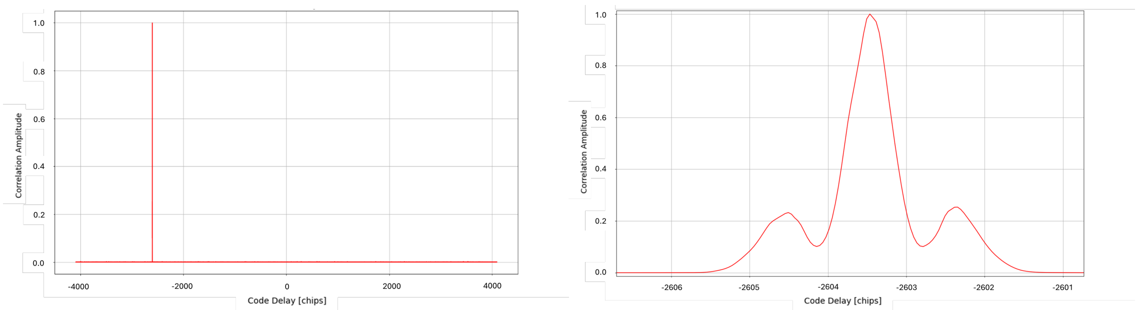

(a) Correlation Function in Code Domain. (b) Zoom Correlation Function in Code Domain.

Figure 2.12: Cross-Correlation Functions of Galileo E1C Signal in Code Domain.

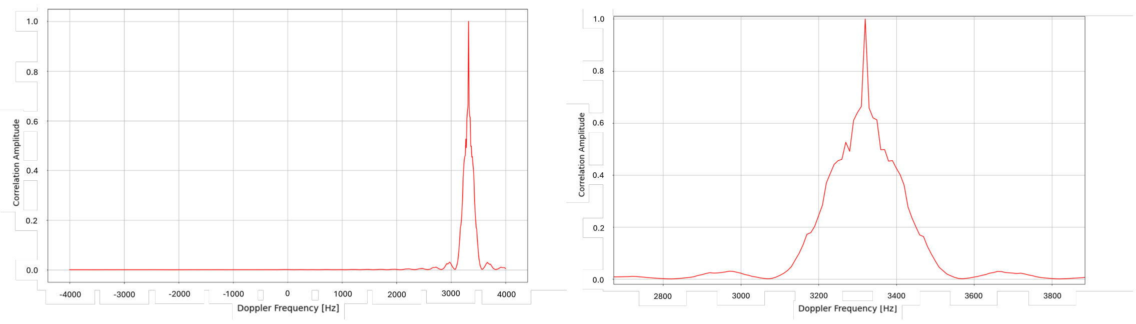

(a) Correlation Function in Doppler Domain. (b) Zoom Correlation Function in Doppler Domain.

Figure 2.13: Cross-Correlation Functions of Galileo E1C Signal in Doppler Domain.

The diagram of a correlation block can be analyzed in Figure 2.14. The RF Front End performs the Analog to Digital conversion, so at the end, it is possible to digitally sample the signal.

The local code is generated according to the code delay input, which indicates by how much the code should be shifted. The Integration & Dump (I&D) block is used so the correlation outputs can be integrated over time [34].

Upon closer examination on the correlation scheme and after the initial mixing stage, the incoming signal from the satellite is modulated with a local oscillator. After that, a low pass filter will make the distinction between w_1 and w_2 waveforms.

Ideally, the correlation would be straightforward if $w_1 = w_2$. However, due to variations in phase between both waveforms, the frequencies do not exactly match. To deal with that, a quadrature mixer is added, introducing two components: In-phase and Quadrature [35].

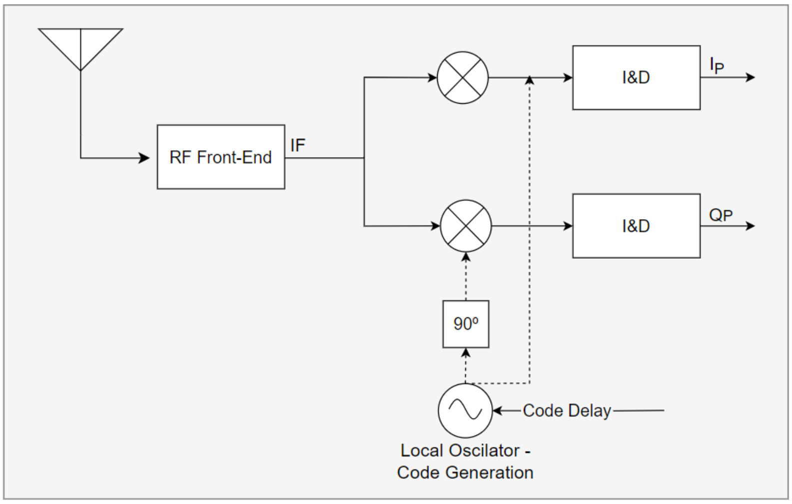

Figure 2.14: Correlation scheme (adapted from [34]).

Acquisition Method

During the acquisition phase, there is a signal search process that includes the estimation of the code phase and the signal's Doppler, which is possible through the analysis of the correlation function. If a peak is obtained with a certain magnitude (achieving a certain threshold, e.g. the carrier to noise estimation), then it is declared that satellite is present in the signal and the values to be estimated (Code delay and Doppler shift) can be obtained through that peak's position [8].

The TTFF will also depend on how long this process will take and can be reduced by using the receiver previous information on the position and almanac data. In that way, there are two different models for the GNSS receiver to start-up [14]:

- Hot/Warm Start-up: when the receiver is powered ON shortly after being turned OFF (or if the position is continuously being tracked), the data regarding the almanac, clock, and previous position is still available. That will significantly reduce TTFF.
- Cold Start-up: when the receiver is powered ON after a long time (or if it is located in a different geographical area), there's no information available. In this case, the receiver will not know which satellites are in view needing to check for the delay and Doppler values of all satellites in order to assess which ones are present, this will result in increases in the TTFF.

Search Space

As already mentioned, the Acquisition stage is about estimating the signal's Doppler and code phase, which is a two dimensional search space (computational sources are saved if the space can be reduced).

There are two search directions: Code Direction and Doppler Direction. The Code Direction resolution should be high enough so it won't miss the correlation peak.

The Doppler Direction should be wide enough so it covers the user velocity, clock information and satellite velocity [8].

As seen in Figure 2.15, each bin has the dimensions of both parameters. The search space time will be increased if a Cold Start-Up mode is set given the need for the receiver to check the whole Doppler and Delay possibilities [14]. A Code Bin, represented by $\Delta\tau$, and a Doppler bin, represented by Δf, compose a cell. The number of combinations for the Search Space process will depend on the modulation being used. Considering a Galileo CBOC(6,1,1/11) signal, it can have 1023 or 4092 chips (range), a code step of 0.3456 chips (for resolution), and a range of $\pm 5Khz$, which will result in an elevated number of combinations (this number can be lower if another modulation with less chips is used, like for GPS L1 C/A). Therefore, searching every bin takes a lot of time and resources will be wasted [36]. To conclude, two main aspects define the size of the search space: Doppler Frequency and Code Phase. More details on the calculations and previously values can be found in [36].

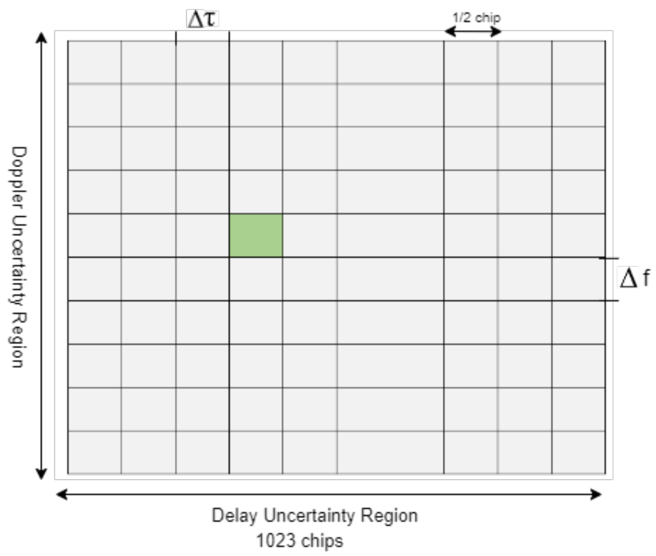

Figure 2.15: Search Space.

2.2.2 Signal Tracking

After estimating the code delay and the carrier Doppler, the tracking stage can be performed. This step will allow to obtain good estimates of the signal parameters. For this process, some filters schemes are commonly used [37]:

- Phase-locked-loop (PLL): for carrier-phase tracking;
- Frequency-locked-loop (FLL): for carrier Doppler frequency shift tracking;
- Delay-locked-loop (DLL): for code delay tracking

These loops have, as a goal, to adjust the input so the local replica signals match with the received signals.

In Figure 2.16, it is possible to analyse a basic block diagram for the tracking loops. The I&D blocks gather correlator's outputs and provide their in-phase and quadrature components. The Discriminator blocks are able to process those outputs and provide the errors from the replica to the incoming signal synchronization (measurable quantities). Then, the filters based on the estimate errors will be able to reduce noise and keep the different values tracked throughout the processing. The Numerical Control Oscillators (NCO) allows the output conversion to usable correction factors of Doppler frequency and code delay [8, 14].

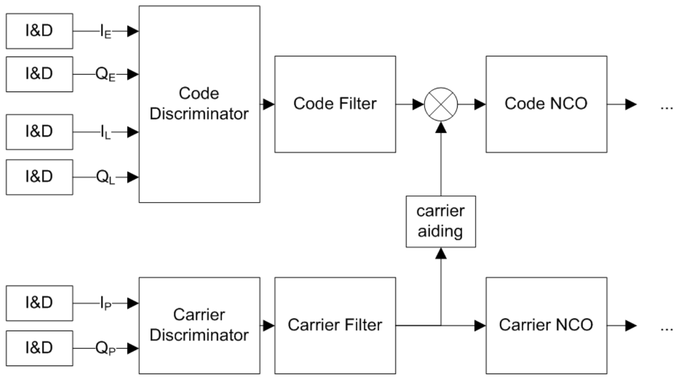

Figure 2.16: Basic diagram for the Tracking Loops [37].

By analysing the bigger picture of a tracking loop architecture it'll be easier to understand how it works. It can be seen in Figure 2.17, an Early-Late Delay Lock Loop (DLL), the most common scheme. This system is built in a feedback system way, being closed by the NCO block. To match the received signal, the adjustment of the local replica signal is achieved through the input of this block.

The process works in the following way: the PRN code is generated with the same phase as the incoming data. To keep on tracking the obtained satellites, the carrier frequency and code phase are maintained in a locked state.

By using the register that produces the three phases (Early, Prompt, Late) of the PRN code, the performance is improved. These three code variations will go to correlators and be multiplied with incoming data, from which the carrier frequency has already been eliminated.

Eventually, and following the diagram, the correlator's output is continuously integrated over one code period. Moreover, after this process of continuous correlation and accumulation, it will be possible to compare the peak value of different phases and acquire correction information that will be sent back to the NCO. New code phases and carrier frequencies will keep being adjusted so the visible satellites are locked [14].

To conclude, in order to ensure the tracking of signals, the receiver is continuously estimating two parameters: Code Delay (to quantify the PRN code replica and satellite's signal misalignment) and the Carrier Phase (defines the relative motion between the satellite and the user - Doppler Frequency) [38].

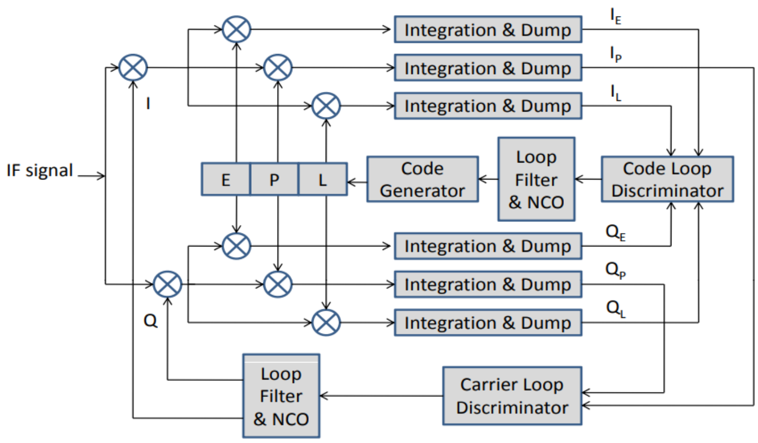

Figure 2.17: Scheme of a DLL Architecture [14].

In harsh environments, the estimation of the previous parameters - Carrier Phase and Code Delay - can suffer degradation. This is especially true in urban areas, where sky visibility is obstructed and buildings cause what is knwon as multipath, which will be explained next.

Multipath Definition

The multipath effect occurs when the signal transmitted from a satellite to a receiver follows more than one path, suffering a delay because of taking a longer and indirect route. This means that the result signal will be a sum of the first path plus the several echoes.

The first signal path, the one travelling directly from the satellite to the receiver without obstructions, is referred as Line of Sight (LOS). The additional signals, the reflected ones, generally arrive later than the LOS and tend to be weaker because of the lost energy during the reflection.

In a simple multipath scenario, the equation for the receiver's input can be described as

$$r(t) = AX(t)\cos\left[(\omega_0 + \omega_d)t + \theta_0\right] + \alpha AX(t-\tau)\cos\left[(\omega_0 + \omega_d)t + \theta_0 + \phi\right] + n(t), \quad (2.11)$$

where α represents the attenuation coefficient of the reflected rays, τ and ϕ are respectively the considered delay and phase errors, and $n(t)$ is the noise [39].

To summarize, the first term of the sum represents the direct received signal, while the second term represents the reflected signals.

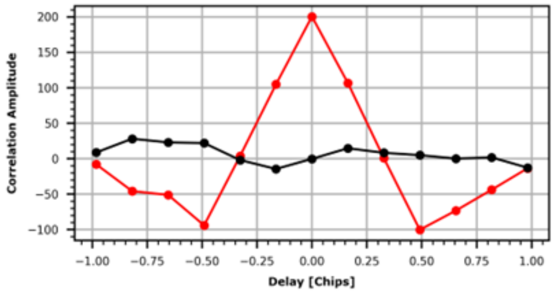

Figure 2.18: ACF without the Multipath effect.

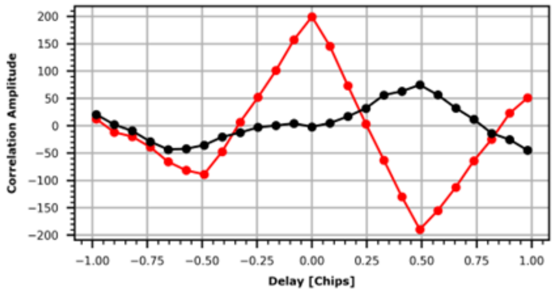

Figure 2.19: ACF with the Multipath effect.

Due to the reflected signals caused by this effect, there is an impact on the ACF, as seen in Figures 2.18 and 2.19. It is possible to observe a distortion when multipath is present, causing the early and late samples to become unbalanced. This can lead to a signal loss of lock, reduced robustness and overall degradation of signal accuracy, making it essential to mitigate this effect in order to improve the GNSS accuracy.

2.2.2.1 PVT Computation

In order to compute the PVT solution two approaches can be considered [40]:

- Least Squares (LS) - The least squares method is a static, deterministic technique used to solve for the receiver's position by minimizing the sum of the squares of the residuals (difference between the measured satellite pseudoranges and the calculated pseudoranges), based on an initial estimate of the receiver's position. All available measurements at a single epoch (moment in time) are processed simultaneously to determine the receiver's position. This method does not save a history of the previous position computations, being the solution in the current epoch independent from the previous one.

- Kalman Filter (KF) - The Kalman filter is a recursive, dynamic estimation technique that considers not only the current pseudorange measurements but also the history of past states (e.g., position, velocity) to provide an optimal estimate of the receiver's position and velocity over time.

In the table 2.3 a comparison between the two different methods is provided.

Table 2.3: LS and KF Positioning Techniques Summary.

	Least Squares (LS)	Kalman Filter (KF)
Nature	Static, batch	Recursive, dynamic
Temporal Dynamics	No (processes on epoch at a time)	Yes (considers past and future states)
Noise Handling	Less robust to noise	Explicitly models noise and uncertainty
Computational Complexity	Simpler but requires multiple iterations per epoch	More complex, but efficient for real-time updates
Estimation Quality	Provides a single best estimate at a time	Provides an optimal estimate over time
Smoothing	Does not smooth over time	Provides smoother estimates due to temporal modeling
Measurement Use	Uses all measurements at once per epoch	Uses measurements incrementally over time

2.3 LEO Satellite Systems

The traditional satellite-based positioning system is based on MEO and Geostationary Orbit (GEO) satellite systems. However, the search for alternatives to improve these systems has been increasing a lot in the past few years given the constant need to overcome the current challenges such as in indoor and some outdoor scenarios due, for example, to multipath [41].

The study of LEO Satellites and their applicabilities has proven to be a promising solution to improve the current systems. Several studies already analyzed the benefits of combining this system with GNSS, but no major practical advances have been made yet for enhancing positioning accuracy and robustness [2].

As outlined on [42] and [1], the following approaches can be used for positioning with LEO satellites:

- LEO as Signals of Opportunity

  These signals are not designed for positioning, although they can be used for that purpose as a positioning opportunity, by using some measurements such as the Angle of Arrival, Received Signal Strength, and Doppler shifts. Some examples of these constellations can be Iridium, ORBCOMM, Globalstar and Starlink. More information and developed studies on these LEO satellite constellations can be found on [1, 41].

- LEO dedicated positioning signals

  As previously mentioned, no constellations for LEO-Position, Navigation and Timing (LEO-PNT) system exist yet. However, studies and plans to implement such a system exist, and an example can be found in [43]. In the paper, it is mentioned that LEO satellites, by being 20 times closer to the Earth and having a rapid geometric change, can contribute to an enhanced Position Dilution of Precision (PDOP) value and a better accuracy and convergence of Precise Point Positioning (PPP). Although the approach could be using LEO satellites as an independent solution, this Thesis will focus on the combined LEO and GNSS perspective, given the need to have an extended amount of LEO satellites to provide full coverage (independently) and to also use the already functioning satellites from GNSS.

During the development of this Thesis, the last presented approach - LEO dedicated positioning signals - will be followed given its highly promising potential to achieve better positioning results when GNSS and LEO operate together. This collaboration is also expected to achieve superior outcomes while ensuring cost-effective investments.

2.3.1 LEO-PNT dedicated

LEO Satellites offer enhanced signal strength due to their proximity to Earth, which makes them particularly attractive for PNT solutions, commonly referred to as LEO-PNT [1, 42].

Finding ways to improve PNT robustness has been increasingly studied due to the need to provide higher positioning accuracy for users and services (particularly in automation fields) and to address insecurities such as spoofing.

GNSS operates at medium to high orbital altitudes, which leads to low signal power (weak signal reception), vulnerability to interference, and difficulties in harsh environmental conditions [44]. This thesis will be focused on two of this environments:

- **Indoor:** The energy and signals are spread out due to the MEO satellites' distance from Earth, resulting in attenuation. These challenges are even more emphasized when referring to indoor conditions. This way, with the addition of the LEO satellites, more measurements will be available with also a higher power (due to the lower distance to earth) helping to mitigate the previously stated challenges.
- **Multipath:** Signal whitening and high Doppler shift, can contribute to the mitigation of multipath, due to the high variation of the satellite position since signals are no longer seen as static over a short duration of time. This way a reflected ray will be much shorter in time than when considering MEO satellite signals.

A study developed by [43] demonstrates significant results when combining LEO satellites with the Beidou system, revealing improvements in both PDOP and satellite visibility.

PDOP describes the ratio between the error in user position and satellite position. It takes into account the geometry of satellites and the lower the value is, the better.

When it comes to satellite visibility, the previously mentioned study, [43], concluded the following: with 3GEO+3IGSO+24MEO the minimum number of tracked satellites was 7.6. However, after adding 120 LEO Satellites, that number increased to 10.1. Additionally, the average number of tracked satellites has a significant increment as well, rising from 10.7 to 16.3 visible satellites. Regarding the obtained results on the PDOP, which is an indicator for the position accuracy, and considering the same constellation, the value for the maximum PDOP reduced from 2.24 to 1.93, and the minimum from 1.63 to 1.22.

Transitioning to an analysis of satellite-related economic aspects, the subsequent Table 2.4 provides insights on the costs of production, launch and annual expenses, along with the number of satellites produced and the expected lifetime for LEO, MEO and GEO satellites [45].

Table 2.4: LEO, MEO and GEO - Economic Aspects.

	LEO	MEO	GEO
Product Cost per Satellite ($MM)	15 to 40	250 to 400	500 to 1900
Launch Cost per Satellite ($MM)	80 (for 6 satellites)	240 (for 1 satellite)	240 (for 1 satellite)
Average Annual Costs ($MM)	410 to 770	390 to 510	200 to 570
Number of Satellites Produced (over 30 years)	432	24	8
Expected Lifetime (years)	5	10	14

When compared to MEO and GEO, LEO satellites have the lowest cost per Satellite. However, given the necessity for a higher quantity of satellites needed to provide continuous coverage, the overall constellation cost is higher. Additionally, the increased frequency of maintenance and the lower expected lifetime for these satellites adds to operational expenses.

2.3.2 Challenges of LEO-PNT Dedicated

When using LEO Dedicated some challenges might be faced [42, 45]:

- **Signal Design:** Choosing the right parameters such as the carrier frequency, bandwidth, modulation, channel coding, multiple-access schemes, and beamforming is an important part to take into consideration when designing these systems, given the fact that the layers - carrier wave, code, and data - will continue to be used to build the signal. LEO-PNT systems may have compatibility with the current developed systems, contribute to enhanced robustness and improve positioning accuracy.

- **Ground Segment:** Receivers must be able to handle challenges related to the substantial Doppler range/shift resulting from the rapid movement of these satellites. LEO satellites can complete one Earth revolution in a couple of hours, which means that signal measurements need careful consideration. For instance, the acceleration and the Doppler shift vary along the LOS with the satellite's elevation angle.

- **Economic Aspects:** As analyzed in Table 2.4, when designing and planning the orbit involving LEO satellites, a consideration between all these factors needs a balanced trade-off. However, if LEO satellites had a significant price reduction per unit, due to an elevated production quantity, their cost could get closer to MEO and GEO.

Chapter 3

Design and Definition of the LEO Satellites System

3.1 Basic Link Analysis and Link Budget

In a Satellite Communication System, or in any Communication System, the evaluation of its performance is an important analysis which provides insights into the signal parameters (transmitted and received power, receiver sensitivity, noise and interference, etc) [46].

This way, in order to assess the impact of LEO satellites for PNT, it is mandatory at a first stage to define the system, since at the day of this Thesis does not exist any dedicated LEO constellation for PNT.

Considering that, the following section presents a description of the different design choices proposed for a dedicated LEO constellation for PNT purposes. Most of the defined parameters were based on existing PNT constellations in MEO, such as GPS, Galileo, BEIDOU, and also on existing LEO constellations for other purposes, like monitoring for example. This Chapter will go through the fundamental aspects to be taken into account when performing a Satellite Link Design analysis, such as the transmitted/received power, frequency band, general orbital parameters, modulation, etc.

3.1.1 Parameters and Components Determination

When performing a Satellite Link Analysis, some properties are being determined, such as: transmitted and received power, frequency band, general orbital parameters (Keplerian parameters), number of visible Satellites, modulation, antenna gain, propagation losses, etc.

Considering the outlined goals in this Thesis, some parameters are defined by default by the Skydel Software, meeting the requirements while being aligned with the analysed scenarios.

3.1.1.1 Constellation Design

Constellation design allows to define and distribute strategically several satellites, sharing similar characteristics, across one or more orbits.

The study presented in [47], delves into several options for optimized hybrid LEO constellations, particularly for LEO-based navigation system, aligning closely with the objectives of this Thesis. It explores several possible schemes of constellation configurations and analyses the obtained results for each.

For efficiency purposes the proposed constellation scheme was not fully implemented in this Thesis. Instead, it was used an orbit of an existing LEO constellation, Starlink. Still, the theoretical insights gained from this study provide valuable guidance for future research and practical applications. Additionally, the study was mandatory and important to determine if the chosen TLE's orbit were feasible and in line with a possible LEO constellation for PNT.

In the referenced Thesis [47], a careful analysis was made in order to determine the optimal number of LEO satellites required to achieve globally even coverage with 6 visible satellites in every instant for different elevation mask angles: 7º, 15º, and 20º. For that purpose, the constellation type was fixed to a hybrid orthogonal circular-orbit/Walker constellation.

The results of this analysis are insightful for theoretical exploration and can be seen in Figure 3.1, which shows the penalty values for each scheme.

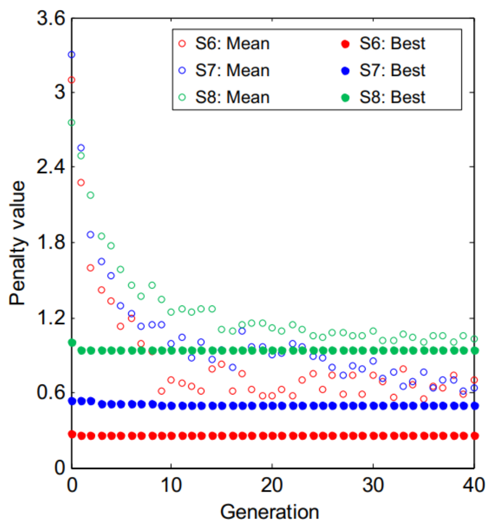

Figure 3.1: Traces of the penalty values for S6, S7 and S8 [47].

From all the presented schemes, S7 seems to be the most balanced option due to its favorable compromise between coverage and penalty value and its technical advantages. This scheme, which uses an elevation mask of 15º and 6 visible satellites on average, requires a total number of 172 satellites. Such configuration ensures global coverage and offers a significant redundancy, enhancing the system's resilience against any individual satellites failures and ensuring continuous and reliable coverage. Moreover, the increased number of visible satellites in this scheme can improve location accuracy as it allows for a better diversity of lines of sight, leading to a better GDOP. Therefore, the choice of 172 satellites is theoretically ideal for balancing the requirements of coverage, accuracy and resilience in a LEO-PNT system [47].

While the mentioned constellation scheme analyzed previously was not implemented in this Thesis, these theoretical insights influenced the decision to use a Starlink constellation for practical simulations, as it aligns closely with the theoretical aspects discussed, offering global coverage, redundancy and high accuracy.

3.1.1.2 Transmitted and Received Power Characteristics

The power received on ground is an important factor in determining the robustness and reliability of the positioning signal. This value, at the ground level, is influenced by several factors, including the transmitted power, free-space path loss and atmospheric attenuation. Due to the LEO satellite's proximity to Earth, less signal attenuation and slightly higher received maximum power are expected, compared to MEO satellites.

Considering user elevation angles above 5 degrees, the expected value for the total received minimum power can be considered the same as for the Galileo satellites, which is -155 dbW. Regarding the total received maximum power, a value of -150 dbW is typically considered for Galileo satellites. However, due to the lower orbital altitude and reduced atmospheric attenuation associated with LEO satellites it was determined to add an additional 2dB, resulting in a maximum received power of -148 dbW [11].

It is important to emphasize that the focus is not necessarily on achieving higher received power levels on ground, but rather on leveraging the proximity of LEO satellites to Earth to reduce their technical requirements. This means that, with less demanding transmission characteristics, LEO satellites can ensure power levels on ground equivalent to those of the Galileo system.

3.1.1.3 Transmission Losses

Although for simulation purposes propagation losses were not taken into account, it is important to be aware that they exist and affect the quality and reliability of the signal.

The main losses affecting LEO-PNT systems include:

- Atmospheric Losses (Ionospheric and Tropospheric)
- Multipath Losses (signal reflections from surfaces)
- Free-Space Path Loss (spreading of the signal as it travels through space)

The ionospheric layer is the highest one on the atmosphere, and due to sun's radiation, it is full of ionized particles that will cause absorption, propagation delay, frequency changes, dispersion of the signal, etc. The radio waves crossing the troposphere are affected by rain attenuation, fog, clouds, and other factors, which will affect a small percentage of the signal that won't reach the receiver antenna at the ground station.

Regarding multipath, signals coming from LEO satellites have a higher power, which contributes for a better mitigation of this effect. Additionally, by having more satellites available in the sky, makes the recovery of the original signal way easier.

Free-Space Path Loss refers to a decrease of signal intensity as it travels through space. Although LEO signals are closer to Earth, this loss is not that much affected, which can be seen through its equation

$$FSPL = 20\log_{10}\frac{4\pi df}{c}, \tag{3.1}$$

where f is represented in MHz and d in km [48].

Another consideration is that, while LEO satellites orbit within the ionosphere, MEO satellites are above it (as can be seen in the illustration in Figure 3.2). This means that the ionospheric effects on LEO signals are less predictable (due to the variability of the ionosphere), compared to MEO signals. The current correction models used for GNSS may not be entirely valid for LEO satellites and future research is needed to develop more accurate models for this conditions [49, 50].

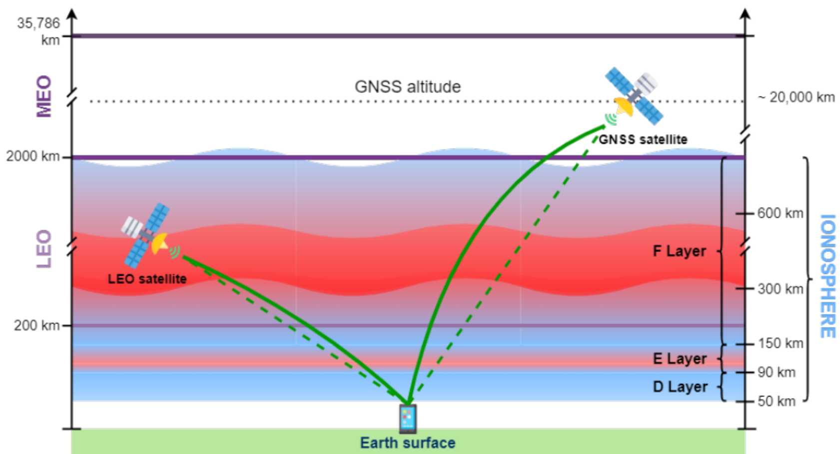

Figure 3.2: Ionosphere layer representation [49].

3.1.1.4 Frequency Band and Modulation

The current GNSS system operates using several frequency bands, as already studied in subsection 2.1.2.

Currently, and given the success of the GNSS, the L-band is significantly congested, which may cause interference or additional attention to where the signal should be allocated to minimize that interference. For the purpose of this Thesis and to implement a LEO satellite system, the selection of the S-band seems the most appropriate choice for several reasons presented below and as it is already analysed in [51, 52].

Firstly, the S-band can be easily compatible with the existent GNSS (due to its proximity with L band), ensuring integration and interoperability, and it is already in use in many countries, namely in ITU Region 3 [52].

Secondly, the propagation attenuation increase with the frequency, and the required antenna input powers are around 2 times larger than it is for the L-band, which is still feasible [51].

Additionally, the S-band propagation characteristics make it particularly well-suited for indoor signal penetrations and some applications like agriculture, when compared to C-band or X-band [53], which is an important detail due to the indoor and multipath scenarios yet to be analyzed further in this Thesis.

Regarding the selection of the modulation scheme for the purposed LEO system, the choice of BPSK(10) presents several advantages.

The BPSK modulation is a robust technique due to the 180 degrees phase shift between the binary 1 and 0, and it is also simple to implement, making it well-suited for satellite communication systems and minimizing computational complexity and receiver requirements [54]. This modulation has no problems with compatibility since this technique is already implemented in the existent GNSS, which facilitates its integration. BPSK also occupies less bandwidth, when compared to a high order modulation scheme for the same data rate. BPSK(10) transmits one bit per symbol while maintaining a good robustness against noise, interference and multipath. Since conserving the bandwidth is an important aspect, due to the high number of allocated frequencies, these characteristics point to BPSK(10) to be a good option.

An additional consideration is to ensure the signal integrity by carefully select the central frequency, given the existence of the BPSK modulation within GNSS. Although the S-band frequency range goes from 2GHz to 4GHz, the Skydel Software, used to generate the signal, exclusively supports the frequency 2492.028 MHz in the S-band. This central frequency selection is good due to its compatibility with the receiver and given the favourable characteristics which include reduced interference and enhanced signal stability within the bandwidth range.

3.2 Testing Phase

In this subsection, the Testing Phase of the LEO-PNT system, previously designed, will be performed. The purpose of this phase is to assess the performance of the system by presenting the scenario final design, simulation dynamics, and signal generation, which will be processed by the receiver.

3.2.1 Scenario Design

To define the constellation design, it is necessary to provide the orbits of the satellites. This can be done through a Two-Line Element (TLE) format file, which is then processed by the Skydel software.

As previously mentioned in subsection 3.1.1.1, the Starlink constellation aligns best with the theoretical aspects and goals of this Thesis. The Starlink TLE was then used to represent the LEO-PNT constellation's orbit parameters. This was accomplished by accessing the `https://celestrak.org/NORAD/elements/` website and retrieving the Element Sets of the current Starlink data.

Further details and analysis on the TLE are following provided.

Two-Line Element Set Format

The TLE format encodes orbital elements of an Earth-orbiting object, describing its trajectory for a given point in time (epoch).

An example of a TLE for Galileo is shown in Figure 3.3:

```
GSAT0203 (PRN E26)
1 40544U 15017A   24197.07194515 -.00000077  00000+0  00000+0 0  9999
2 40544  56.9303   0.7099 0001848 238.4221 121.5721  1.70476272 57897
```

Figure 3.3: Two-Line element set for Galileo [55].

Each line of a TLE has a specific structure and format.

The **Title Line** is optional, and it contains the satellite designation, as shown in Figure 3.4.

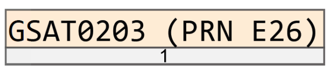

Figure 3.4: TLE Title Line.

Figures 3.5 and 3.6 illustrate the structure of Lines 1 and 2 of the TLE for Galileo, with the corresponding fields and their content description detailed in Tables 3.1 and 3.2, respectively.

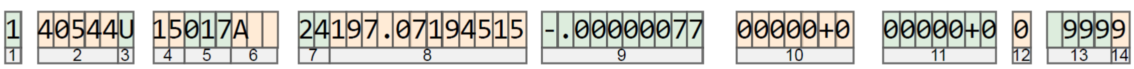

Figure 3.5: TLE Line 1.

Table 3.1: Line 1 structure.

Field	Content
1	Line Number
2	Satellite Catalog Number
3	Classification (U: Unclassified)
4	International Designator (last two digits of launch year)
5	International Designator (launch number of the year)
6	International Designator (piece of the launch)
7	Last two digits of the Epoch Year
8	Epoch
9	First Derivative of Mean Motion
10	Second Derivative of Mean Motion
11	Second Derivative of Mean Motion
12	Ephemeris type
13	Element set number
14	Checksum

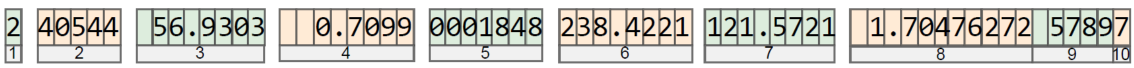

Figure 3.6: TLE Line 2.

Table 3.2: Line 2 structure.

Field	Content
1	Line Number
2	Satellite Catalog Number
3	Inclination (º)
4	Right ascension of the ascending node (º)
5	Eccentricity
6	Argument of perigee (º)
7	Mean anomaly (º)
8	Mean motion (revolutions per day)
9	Revolutions
10	Checksum

3.2.1.1 Scenarios Overview

In this testing phase, several scenarios were evaluated using the GNSS software receiver, XRC, to analyse the performance and added value of using LEO Satellites.

The three main scenarios, their definitions, and purpose are presented below:

- GAL+LEO Open Sky: This scenario combines both Galileo and LEO satellites in an open sky environment. This means that all 4 quadrants are considered, providing an optimal setup with a rich set of visible satellites. In the current scenario, the LEO constellation is not expected to provide a high added value due to the substantial number of visible Galileo satellites. However, it is important to assess the reference performance and understand how transitioning from the current scenario to indoor and multipath environments affects performance.

- GAL+LEO Indoor: Combines Galileo and LEO satellites under indoor conditions. For the scenario to be considered indoor it is assumed that the first and fourth quadrants are visible (mimicking a scenario in which the satellites are only visible through a window, which is very representative of an indoor scenario).

- Multipath in GAL+LEO: In the current scenario, the focus is to simulate an urban scenario in which a multipath is present (like a city center). The scenario is equal to the GAL+LEO Open sky, but buildings and trees are considered. Consequently, the processed signal will experience multipath impairment, which can be observed through indicators like degradation in the Carrier-to-Noise-Ratio (CN0).

It is important to note that, for each scenario analysed, only satellites above 5º elevation are considered, as this threshold ensures more realistic conditions, both in indoor and outdoor environments. In typical conditions, signals coming from satellites below this elevation are often obstructed or not visible, making them unavailable for processing.

3.2.1.2 Simulation Dynamics and Signal Generation

In this section, the dynamics of the simulation, including the signal generation, will be presented.

During this phase, the complete scenario was created, using the Skydel Software, which is a GNSS simulation tool offering multi-constellation/multi-frequency signal generation [56]. The main scenario incorporates both Galileo (MEO satellites) and LEO satellites, considering the four quadrants visible. From now on, this specific scenario will be referred as "**GAL+LEO Open sky**".

The process and configuration aspects used to develop the scenario will now be analysed.

For the simulation purposes, the receiver was considered fixed/static, with the following coordinates:

- Latitude: 6.55180000º
- Longitude: 152.74400000º
- Height: 2.0000m

These specific coordinates were chosen based on a previous analysis of that particular location and start time (GPS Time: 2024-05-15 10:16:00), ensuring that, as previously designed, multiple satellites were visible in the sky, providing representative results for the future LEO constellation. By carefully selecting the time and location with representative satellite visibility, the results become more reliable, allowing us to obtain better data and results.

For the purpose of this simulation, a TLE from Celestrak [55] for LEO Satellites (Starlink) was injected, as previously stated in subsection 3.2.1.

As mentioned in subsection 3.1.1.4, the chosen modulation for the new LEO signal was defined as being a BPSK(10). In order to achieve the signal, a Custom Signal, based on the L5Q (BPSK(10)), was created. To be in line with the defined system (via the Custom Signal plug in) the central frequency was defined in the S-band as 2492.0280 MHz, instead of the L5Q native central frequency of 1176.45MHz. With the previous understanding, it is possible to simulate the LEO constellation taking into account all of the assumptions and design decisions presented in previous subsections.

At this point, two signals are being used: Galileo E1 and LEO L5Q_S.

The obtained visible satellites are shown in Figure 3.7.

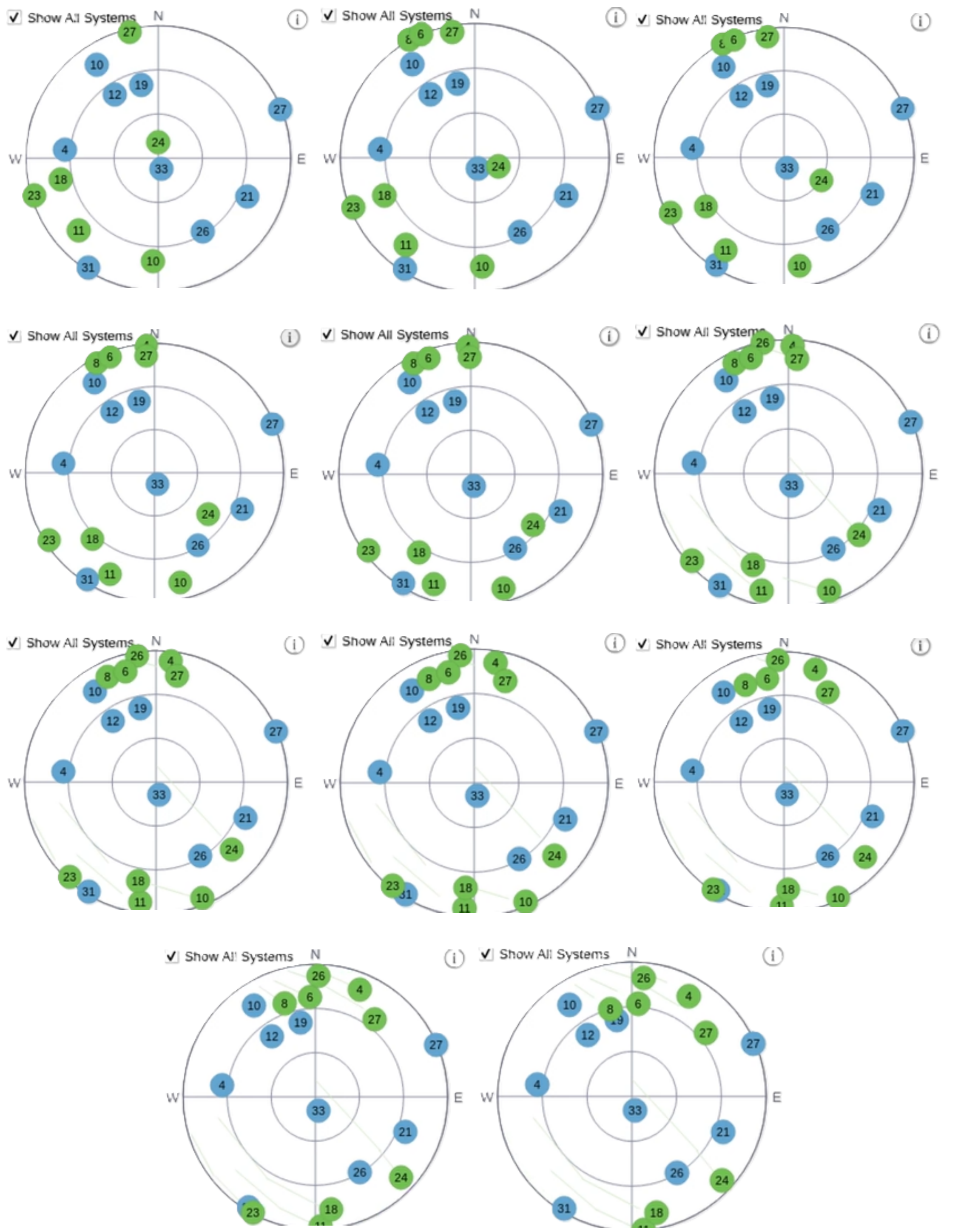

Figure 3.7: Sequence of frames showing satellite displacement over time (every 30 seconds).

It is evident from the figures that while the MEO satellites, represented by the blue color, appear to remain relatively stationary (not moving), there is a noticeable difference with the LEO satellites, represented by the green color. These satellites, due to its orbits, show a significant distance traveled and changes in position every 30 seconds. As will be discussed later, this increased movement, velocity, and rapid shifts in position, have a substantial impact on the processing of tracking loops and the overall performance at the receiver level.

The obtained elevation, azimuth and range (at a 60 seconds rate), corresponding to the available satellites in the open sky scenario, are presented in the following Table 3.3.

Table 3.3: Time series Open Sky.

	Elev (º)	Az (º)	Range (m)	Elev (º)	Az (º)	Range (m)	Elev (º)	Az (º)	Range (m)	Elev (º)	Az (º)	Range (m)
Time (ms) / SV ID	500			60000			180000			300000		
E4	26,65311	-85,14931	26184751.5026	26,66547	-84,71382	26183649.15322	26,68644	-83,83579	26181782.38425	26,70224	-82,95825	26180379.23548
E31	1,878713	-147,9028	28685933.41774	1,99713	-148,1743	28672822.6028	2,241526	-148,719	28645789.45754	2,493377	-149,2595	28617967.71186
E12	38,23749	-34,57904	25224726.92547	38,56359	-34,80386	25200182.37323	39,2191	-35,27373	25151262.5568	39,87144	-35,76608	25103138.17557
E27	0,903684	68,493021	28804258.81639	0,883026	68,14944	28806609.86054	0,836503	67,45811	28811890.99107	0,783411	66,76907	28817901.99315
E21	23,46907	113,14555	26474557.21432	23,58368	112,7478	26463923.88872	23,81325	111,9425	26442667.70956	24,04051	111,133	26421682.48699
E26	31,35112	148,32887	25770430.39595	31,02049	148,5224	25798364.82581	30,3528	148,9005	25855177.44046	29,6841	149,2624	25912606.82355
E19	39,61217	-12,80004	25124594.4523	39,40968	-12,43123	25139565.80512	39,00477	-11,69091	25169665.7692	38,60457	-10,95504	25199625.60087
E10	14,65664	-33,54458	27326441.73956	14,95974	-33,6363	27295618.5741	15,57083	-33,83101	27233720.00878	16,18152	-34,03889	27172195.62047
E33	82,10927	161,64767	23260984.33367	81,68612	162,7897	23266208.23313	80,82438	164,7731	23277689.98927	79,95403	166,4158	23290433.62565
L26	-	-	-	-	-	-	2,790474	-8,243907	2385366.24584	10,75892	6,538769	1740300.211708
L04	-	-	-	0,172957	-6,544971	2678677.467134	6,692128	7,016166	2055435.252577	13,14143	30,4157	1613381.479934
L27	2,710857	-12,36276	2412207.452596	6,615133	-7,101918	2060700.19213	16,41122	11,48799	1441958.189988	24,50528	50,54663	1132884.338541
L10	19,78995	-177,5962	1319832.013387	13,72785	170,833	1606060.913532	4,256787	158,1448	2294891.487294	-	-	-
L18	22,30337	-102,5016	1227415.757466	26,37679	-124,3938	1100473.193178	20,85618	-169,8579	1279185.571995	9,831761	167,4285	1848576.828305
L11	16,70794	-132,7842	1411403.140704	14,31665	-149,5628	1530256.981614	6,903042	-172,6516	2018648.560362	0,029236	174,7463	2674649.714502
L08	-	-	-	1,833498	-28,31081	2480476.647381	11,56523	-24,56959	1687964.967535	30,83537	-13,55409	956283.5736238
L06	-	-	-	2,193992	-22,39423	2444010.098675	11,73336	-15,06427	1677849.378474	28,43481	5,111327	1011716.469411
L23	2,032769	-107,181	2459796.391605	2,766047	-117,3007	2386282.151744	2,201354	-138,1624	2442555.132813	-	-	-
L24	79,56223	3,2520181	567870.6571344	56,14558	123,2959	661536.7027234	20,22199	131,7243	1303097.300878	6,777593	133,222	2077226.862676

Based on the table presented above, some observations can be made regarding the behaviour of the LEO and MEO constellations satellites.

LEO satellites, represented in green, exhibit significantly different dynamics compared to the MEO satellites, represented in blue. The range values for LEO satellites are considerably smaller, which reflects their proximity to Earth. Additionally, these range values fluctuate considerably over time, indicating the fast movement of these satellites as they enter and move through the orbit. In contrast, MEO satellites show relatively stable range values, as their higher orbits lead to slower movement and less changes in position when viewed from Earth.

The elevation values for LEO satellites also exhibit greater variation compared to the MEO satellites. For instance, satellite L24 show significant changes in elevation in the time frames presented, which reflects their rapid motion across the sky. This is contrasted with MEO satellites, whose elevation angles remain relatively stable (when considering a static user), indicating that they are consistently positioned at higher altitude and moving in a gradual way across the field of view.

Another important aspect worth mentioning, is the appearance and disappearance of satellites in the LEO constellation. Given their lower orbit and rapid movement, LEO satellites enter and exit the visible sky area more quickly than MEO satellites, which remain in view for longer periods. This aspect will have a significant impact on system performance and signal tracking, as the receiver will have to acquire and lock onto new satellites as other pass out of view.

Table 3.4 shows a summary of the generation parameters discussed earlier and used for the desired GNSS scenario.

Table 3.4: GNSS generation parameters [11].

Trajectory	Fixed
Coordinates	Lat: 6.55180000º ; Long: 152.74400000º ; Height: 2.0000m
Period	15-05-2024 10:16:00 UTC + 00:00
Duration	5 min
Constellation	Galileo E1 LEO L5Q_S
Visible Satellites	E04, E31, E12, E27, E21, E26, E19, E10, E33 L26, L04, L27, L10, L18, L11, L08, L06, L23, L24
Central Frequency	Galileo E1C: 1575.4200 MHz LEO L5Q_S: 2492.0280 MHz
Sampling Rate	25.000 MSps
Modulation	Galileo E1C: CBOC(6,1,1/11) LEO L5Q_S: BPSK(10)
Minimum Power on Ground	Galileo E1C: -157.25 dbW LEO L5Q_S: -155 dbW
Maximum Power on Ground	Galileo E1C: -150 dbW LEO L5Q_S: -148 dbW

3.2.1.2.1 Multipath Generation

In order to simulate the multipath scenario it is necessary to provide a time series that will have information regarding the environment of the user. In this case, and according to the multipath definition, it is represented by an extra replica of the signal, which in turn its defined with a phase, code delay and power offset. The generated time series will have this information, which will be injected into the signal and later tracked with the software receiver.

The time series used for the multipath generation was created using the DLR Land Mobile Multipath Channel tool [57]. In this tool, the user can configure the desired environment (urban or suburban), and then all the parameters (like height of trees, size of the road, number and height of buildings) are automatically defined according to it. For the purpose of this Thesis, the urban environment was the chosen option.

Since this tool is not yet prepared to deal with LEO satellite dynamics, different time series had to be created, dividing the simulation into 5 (5 different time series, representing 1 minute each), to more realistically represent the satellite's trajectory. This was necessary because the tool was designed taking into account MEO satellites, in which, for a static user, the elevation and azimuth of the satellites is constant on a 5 minute period. For a LEO satellite this is not true, and 5 different time series were needed in order to update with the correct azimuth and elevation of the satellites in Table 3.3.

This time series are .mat files composed by a set of parameters, such as: a list of all the

SVID (Space Vehicle Identification) to be affected by multipath, and the multipath array itself to be injected in the base signal (phase and code delay offsets). This array contains, for each satellite:

- Values for LOS delay, LOS phase, and LOS attenuation, relative to the LOS base signal.
- Values for ECHO's delay, ECHO's phase, and ECHO's attenuation, relative to the LOS base signal.

This parameters mentioned above are responsible to define the multipath dynamics.

As a result, a set of time series composed of 3 L0S and 10 ECHOS is generated, for each visible satellite and for the configured multipath scenario.

The Skydel will then directly process this time series using the GMV SDXPAND plug in, by injecting the multipath into the base signal.

3.2.1.3 Signal Characteristics and Transmission Parameters

As mentioned above, the Galileo satellites transmit the E1C signal, while the LEO satellites transmit a signal equivalent to GPS L5Q, with a central frequency shift to the S band (2492.0280 MHz).

The GPS L5 signal has two carrier components: in-phase component, L5I, which contains data (navigation messages), and a quadrature component, L5Q, known as pilot, meaning it doesn't carry any data (only the PRN code).

The L5 signal is modulated using the BPSK modulation, whose advantages were already mentioned in subsection 3.1.1.4. This signal (specifically the L5Q component), and all the modernized GPS civil signals, are designed to improve signal acquisition and tracking robustness. The L5Q component uses a primary code length of 10,230 chips, and it is further modulated by a secondary code - Neuman-Hofman code - that reduces interference and allows a higher data bit synchronization within GNSS receivers. The Neuman-Hofman code for L5Q is 20 bits long.

During each PRN code repetition interval (1 ms), the secondary code modifies the PRN sequence (primary code) by either leaving it as it is or inverting it, based of the secondary code value (0 or 1). For instance, for the L5Q Neuman-Hofman code of '0000110000', the first 4 repetitions of the PRN code will be transmitted as the original, while the fifth and sixth will be inverted, and so on [8].

There is always one secondary code chip per epoch of the primary code. Note that epoch represents the duration of N chips. This is illustrated in Figure 3.8.

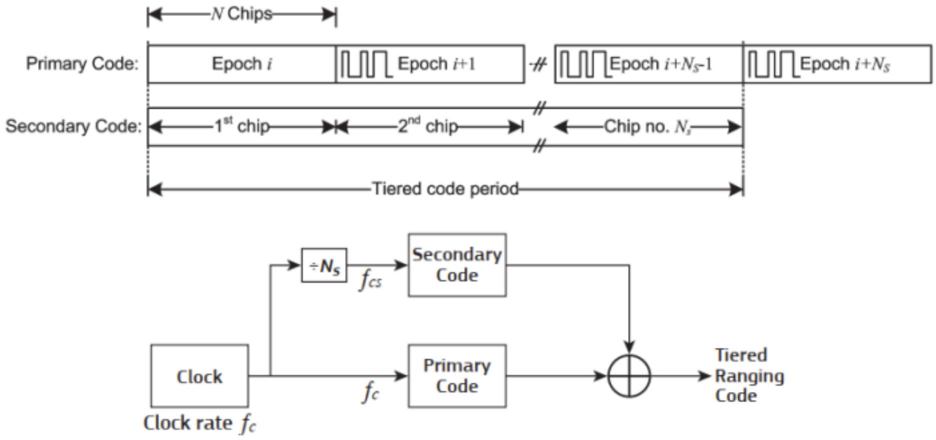

Figure 3.8: Tiered Codes Generation [11].

The power level of the L5Q signal is an important parameter to ensure robust signal reception, especially in challenging environments. The nominal power level for the L5Q signal from GPS satellites is typically around -157 dBW. However, LEO satellites, due to their closer proximity to the Earth, can afford to transmit signals with an additional 2 dB of power (as previously mentioned in subsection 3.1.1.2). This results in a stronger received signal at the Earth's surface, enhancing the signal quality and reliability for end-users [11].

3.2.1.4 Signal Output Generation

In this subsection, the outputs generated through Skydel are discussed, specifically the IQ data and RINEX files, which are crucial outputs for further processing and analysis on the receiver side (xrc - experimental GMV receiver). Figure 3.9 shows a screenshot from the Skydel interface, representing the outputs for both signals, LEO L5Q_S and Galileo E1C.

Figure 3.9: Skydel output with signal configurations.

The In-phase and Quadrature (IQ) file is generated with the .iq extension, 16-bit IQ samples in binary format and has a sampling rate of 25.000 MSps. The Receiver Independent Exchange (RINEX) format is the international standard to store and exchange GNSS data, enabling interoperability between different receiver brands, while having an easy readable form.

The Skydel generates this file which contains information about satellite orbits and other essential parameters (satellite ephemeris, clock corrections, observation data) in a nominal format. An example of a RINEX file can be seen in Figure 3.10. The RINEX files play a crucial role in the receiver's processing stage by providing the necessary aiding data for initial acquisition and tracking of satellite signals [58, 59].

In summary, while the IQ data provides the received satellite signal in binary formats, the RINEX files offer information for aiding signal acquisition and tracking.

```
     3.03           N: GNSS NAV DATA    E: Galileo          RINEX VERSION / TYPE
SKYDEL              SAFRAN              15-May-24 10:16     PGM / RUN BY / DATE
                                                            END OF HEADER
E02 2024 05 15 10 00 00 6.264128023759E-05 2.941646926047E-12 0.000000000000E+00
     1.000000000000E+00 4.037500000000E+01 3.408356257433E-09 2.326321864279E+00
     1.942738890648E-06 2.830476732925E-04 2.764165401459E-06 5.440612394333E+03
     2.952000000000E+05 1.676380634308E-08 2.107660743033E-01 2.235174179077E-08
     9.682402232060E-01 2.843125000000E+02-3.736688537676E-01-5.916675024692E-09
     3.160845947635E-10 3.000000000000E+00 2.314000000000E+03 0.000000000000E+00
     3.120000000000E+00 0.000000000000E+00-4.656612873077E-10-1.164153218269E-09
     9.999000000000E+08 0.000000000000E+00 0.000000000000E+00 0.000000000000E+00
E03 2024 05 15 10 00 00-5.580455763265E-05-3.709033080668E-12 0.000000000000E+00
     1.000000000000E+00-1.634062500000E+02 3.154774266154E-09-3.061113992346E+00
    -7.588416337967E-06 3.221911611035E-04 7.405877113342E-06 5.440620018005E+03
     2.952000000000E+05 5.029141902924E-08-1.886235878754E+00-4.284083843231E-08
     9.595140616921E-01 1.850937500000E+02 7.715437381679E-01-5.718809639948E-09
    -6.200258265644E-10 3.000000000000E+00 2.314000000000E+03 0.000000000000E+00
     3.120000000000E+00 0.000000000000E+00 3.026798367500E-09 3.492459654808E-09
     9.999000000000E+08 0.000000000000E+00 0.000000000000E+00 0.000000000000E+00
```

Figure 3.10: RINEX Example File.

3.2.2 Receiver Processing

XRC (eXperimental Receiver Canvas [60]), is the GMV experimental receiver, that is able to process multiple signals in different scenarios and approaches. It has a high array of possible configurations and expansion capabilities, which allows to design and evaluate the performance of innovative GNSS processing algorithms. The experimental receiver is scalar, from a computational processing point of view, allowing to operate and run in low specifications laptops, but also in high end components, since it explores the available hardware resources. The main difference will be the processing times and capabilities, in terms of the tracked channels.

The software receiver is also able to generate Signal quality monitoring (SQM) metrics which makes it the ideal solution for performance assessment and implementation of innovative techniques, as is the case of the current Thesis, in which new signals need to be tracked (S-band).

The main inputs of the receiver are the IQ file, which has the signal to be processed and correlated, and the RINEX files to aid in acquisition and re-acquisition. Finally, the configurations, which allow to select the desired constellations/satellites/bands/modulations with a high degree of flexibility.

3.2.2.1 Fine-Tuning

The signal processing begins with the acquisition phase. If a signal is detected, it enters the FLL while keeping on checking the code lock (synchronization between locally generated and received satellite signal's code). Once the code and frequency are locked, the FLL will be switched to a PLL tracking, providing the correct carrier phase value enabling carrier positioning. If the receiver loses the lock of the phase, the tracking continues but only with carrier doppler tracking, through the FLL, not providing accurate phase estimates. In the case both code and phase lock are lost, the acquisition phase starts all over again, which is refereed to re-acquisition [8].

To successfully process the incoming LEO signal, an implementation had to be performed in the experimental receiver. Since the signal was newly designed in the scope of this Thesis, the receiver was not prepared to handle it and a new central frequency signal had to be generated in order to successfully correlate it with the incoming LEO signal.

Additionally, a fine tune at the configuration level was mandatory in order to handle the different characteristics of the LEO signal when compared with the nominal MEO satellites. This is especially true for the satellite dynamics, which will have a big impact on the tracking loop filters as will be shown next.

Table 3.5 presents the summary of configurations used in the software receiver.

Table 3.5: XRC configuration parameters.

Configuration	Value		Description	
	L5Q_S BPSK(10)	E1C CBOC(6,1,1/11)		
Mask Angle [ª]	5		Satellite elevation mask	
Sky Scan Period [s]	10		Receiver period of operation of updating visible satellites	
Sampling Frequency [MSps]	25		Sampling frequency / rate	
C/N0 [db-Hz]	35		Acquisition	Threshold for C/N0
Coherent and Non Coherent Integration Time [s]	$20e^{-3}$	$100e^{-3}$		Duration of which the signal is integrated
C/N0 Loss of Lock [db-Hz]	25		Reacquisition	Threshold for C/N0 Loss of Lock flag
Phase Lock	65º			Phase error to assume loss of lock (degrees) - PLL
Time to declare Loss of Lock [s]	4			Threshold of the time to declare loss of lock
Coherent and Non Coherent Integration Time for reacquisition [s]	$20e^{-3}$	$100e^{-3}$		Duration of which the signal is integrated during reacquisition
Coherent and Non Coherent Integration Time for tracking [s]	$1e^{-3}$	$4e^{-3}$	Correlation Process	Duration of which the signal is integrated during tracking
Bandwidth PLL	45	15	FPLL Carrier Filters	Phase-locked loop bandwidth
Bandwidth FLL	5	1		Frequency lock loop bandwidth
Bandwidth DLL	5	1		Delay lock loop bandwidth
Order PLL	3	2		Order of the PLL Filter
Order DLL	3	2		Order of the DLL Filter
Phase Lock FLL (º)	65º			Phase error to assume loss of lock to activate FLL
Discriminator PLL and FLL	ATAN2			Type of Discriminator

By analysing the previous table, it is clear that the main fine tune at tracking level was performed in the phase lock loop.

The decision to use a third-order instead of a second-order filter to track LEO satellites, is primarily due to the dynamic nature of these satellites, when compared to MEO satellites (such as the ones in the Galileo constellation).

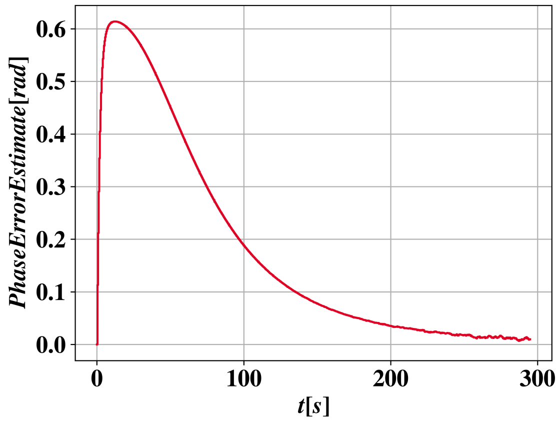

Figure 3.11: Second Order PLL Phase Error Estimate.

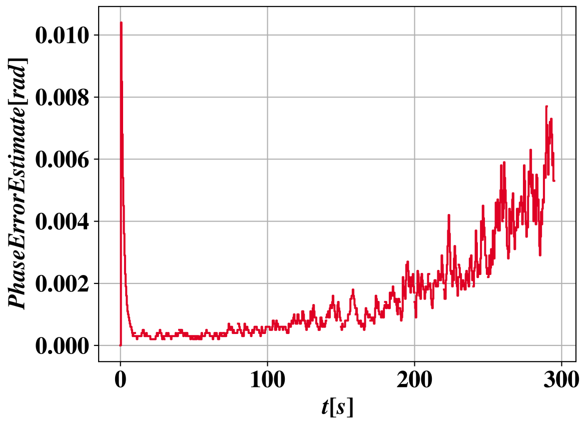

Figure 3.12: Third Order PLL Phase Error Estimate.

As it is possible to analyse from Figures 3.11 and 3.12, the phase error estimate for a second order PLL shows an initial high error value, which gradually decreases over time. However, despite reaching a low phase error value, this PLL takes a considerable amount of time to stabilize, specially given the dynamic nature of LEO satellites. Additionally, it is evident, by the slow curve's descending, that the second order PLL struggles to track the rapid motion and velocity changes of LEO satellites, not being able to lock on the phase.

On the other hand, Figure 3.12 shows the phase error estimate for a third order PLL. The main difference lies in the behaviour of the error over time. This PLL starts with a lower phase error, maintaining a stable phase lock over the entire observation period. Despite some variations, the overall phase error remains significantly lower compared to the second order PLL.

Third order PLL are specially designed to deal with acceleration, which is a critical factor when dealing with LEO satellites. For that reason, by using a third order PLL, the receiver is able to adapt to maintain a signal lock [61].

To provide more information and context on the PLL, a brief explanation is presented below.

Basics of a PLL architecture

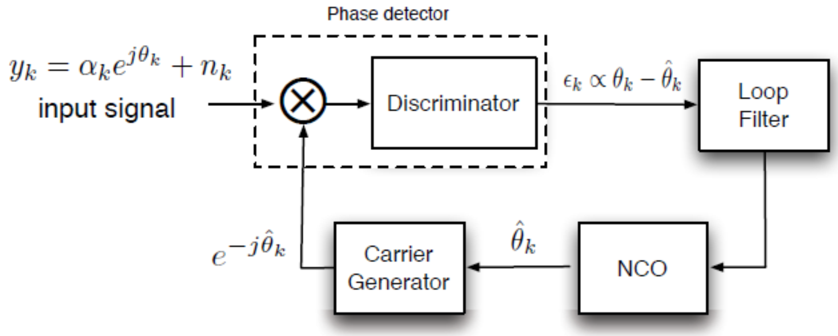

Figure 3.13: PLL standard architecture [62].

On a standard PLL architecture, illustrated in Figure 3.13, there are three main blocks: the phase detector, the loop filter, and the NCO block (an integrator). The phase detector's output represents a phase estimation error, which goes through the loop filter that will drive that error to zero and filter out the noise, while the NCO is responsible to generate the local replica.

The loop filter attenuates the phase error due to the Doppler frequency shift, caused by the motion. As analysed on [61], the steady state (difference between the input and output) error is not zero under high dynamic conditions and a wider bandwidth is needed in order to that error converge faster to zero.

The third-order PLL comes to solve this problem and its elements are a phase detector, VCO and a loop filter with external velocity aiding and feedback.

3.2.3 Analysis of Results and Added Value

In this section, the results of the previously described scenario are presented in order to retrieve the added value that the proposed LEO constellation will provide. For this, an analysis will be made in order to evaluate both the final positioning accuracy (the error is assessed based on the real reference position) and the performance of the signal tracking loops, in terms of its power during the processing and the estimates of the code delay, which will be translated into a position in the PVT engine.

3.2.3.1 Reference Scenario - Open Sky

3.2.3.1.1 Tracking Loops Performance Analysis

In the following sections, the Open Sky scenario is presented. This scenario is essential to assess the performance and will serve as a reference when analyzing the obtained results in the indoor and multipath environments. As previously specified, the key difference between these two scenarios is that, in indoor environment, only two quadrants are considered, while there are four for the open sky scenario. As a result, fewer satellites are available for analysis in indoor scenario. This can be seen in Figures 3.14(a), 3.14(b), 3.15(a), and 3.15(b), representing the sky plot for both scenarios.

Due to the low number of Galileo satellites in the indoor scenario, it is already clear that relying solely on the Galileo constellation will not provide a position solution. This highlights the significant added value of the LEO constellation, which makes it possible to obtain a position solution, as will be demonstrated in the analysis of the indoor scenario.

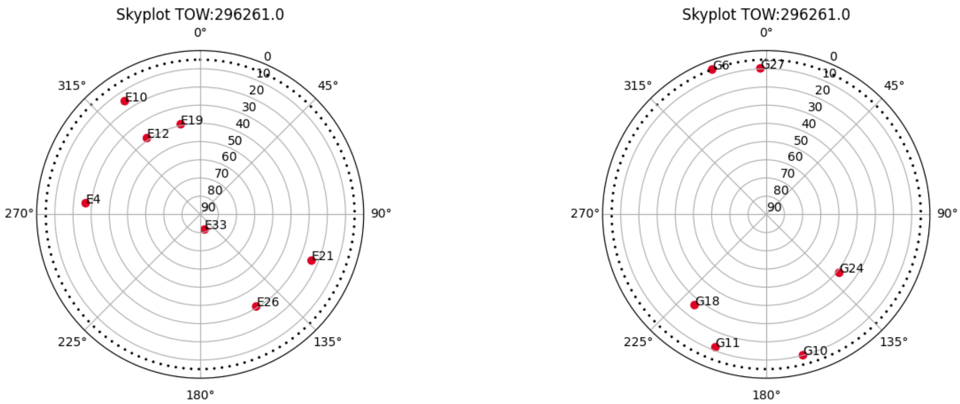

(a) SkyPlot Open Sky - MEO Satellites. (b) SkyPlot Open Sky - LEO Satellites.

Figure 3.14: SkyPlot of MEO and LEO visible Satellites for the open sky scenario.

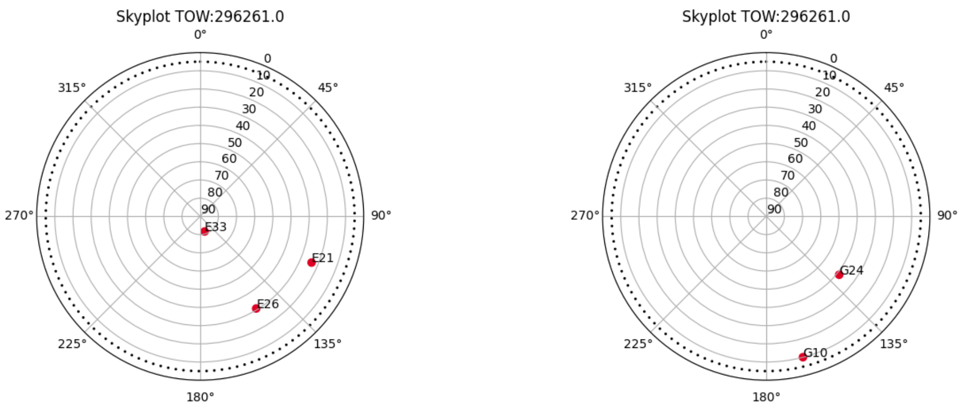

(a) SkyPlot Indoor - MEO Satellites. (b) SkyPlot Indoor - LEO Satellites.

Figure 3.15: SkyPlot of MEO and LEO visible Satellites for the indoor scenario.

Open sky: LEO + Galileo satellites

Following is presented the performance analysis of the tracking loop estimates for the considered satellites. The analysis will focus on the estimated CN0, doppler and code delay, because these present a meaningful overview of the receiver performance. The code delay estimates are tied to an ambiguous pseudorange, meaning that the noise in these estimates will have an impact in the overall position solution. Keeping track on the Doppler is crucial, especially with the LEO constellation, since new dynamics will be present, making it an essential parameter for a comprehensive and full view of performance. Finally, the CN0 offers a clear indication if the signal tracking is being performed correctly, gathering the expected signal power from the signal tracking.

The carrier-to-noise density ratio (CN0), expressed in (db-Hz), is an important metric used to evaluate the strength and quality of a signal, indicating its clarity, and is defined as the ratio of the received carrier power to the noise power.

Figure 3.16 and Table 3.6 depict the carrier-to-noise ratio estimation of the different satellites and their respective mean values.

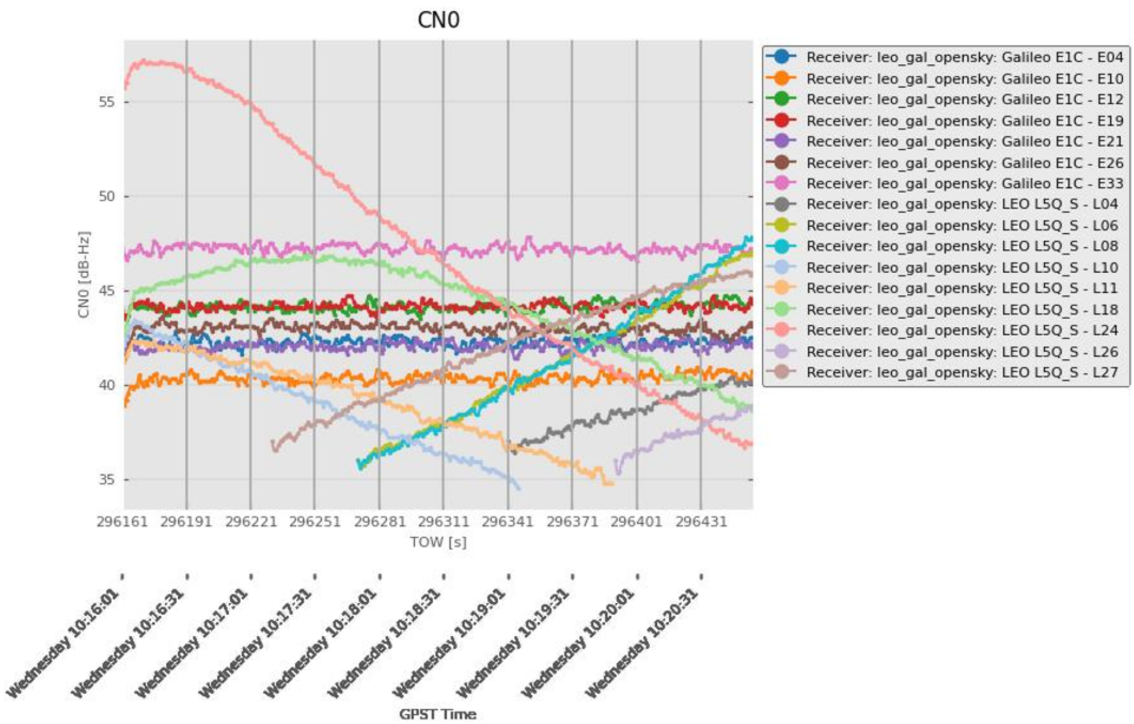

Figure 3.16: CN0 results.

Table 3.6: CN0 - Mean results.

CN0 - Mean [db-Hz]	E04	E10	E12	E19	E21	E26	E33	L04	L06	L08	L10	L11	L18	L24	L26	L27
E1C	42.267	40.341	44.123	44.16	42.04	42.987	47.209	nan	nan	nan	nan	nan	nan	nan	nan	nan
L5-Q	nan	nan	nan	nan	nan	nan	nan	38.6	41.221	41.305	39.027	39.151	44.165	47.105	37.418	42.0

Due to the high range of motion of LEO satellites, it is common to experience signal loss of lock when the satellite's elevation decreases below the configured elevation mask of 5 degrees, which is the main reason why not all the signals have a doppler estimate contemplating the full simulation time of 5 min. Additionally, discontinuities are often observed when a satellite enters (for the TOW of 296341 s, the satellite L04 becomes visible) or exits the visible sky (L10 exits the visible area approximately at a TOW of 296350 s).

As expected, the maximum value of CN0 is achieved when a satellite is at its highest elevation (close or at the zenith point) and that value decreases and gets noisier with low elevation angles. Moreover, it is easy to distinguish LEO from MEO satellites by observing the variations on the CN0 values, in which they seem constant for the Galileo constellation when compared to the LEO satellites.

As previously mentioned, propagation losses play a significant role, where the received power on Earth is a function of the distance between the receiver and the satellite. Since this distance has more variation for LEO satellites, due to their rapid movement across the sky, the received power fluctuates significantly as well. In contrast, for MEO satellites, where the orbital periods are much longer, a similar behaviour to what is observed over 10 minutes for LEO satellites would only be noticeable over several hours for MEO satellites. This highlights the faster changes in signal strength and dynamics with LEO satellites.

A detailed observation on this type of behaviour can be found on Figures 3.17 and 3.18, for LEO satellite 24 and Galileo 33, respectively.

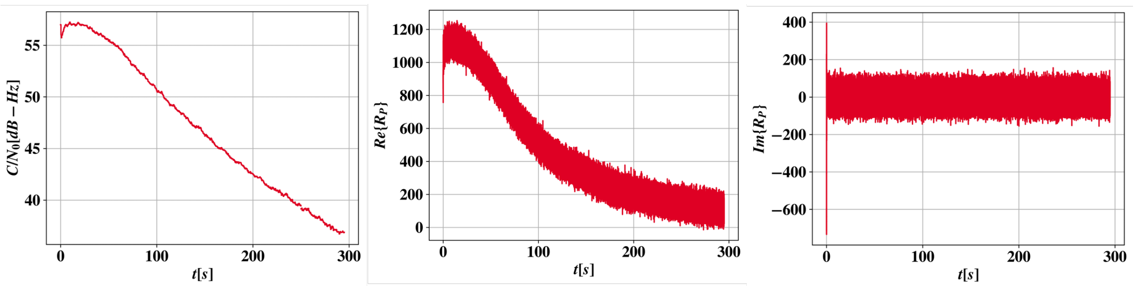

Figure 3.17: L24 - CN0, real, and imaginary part results variation.

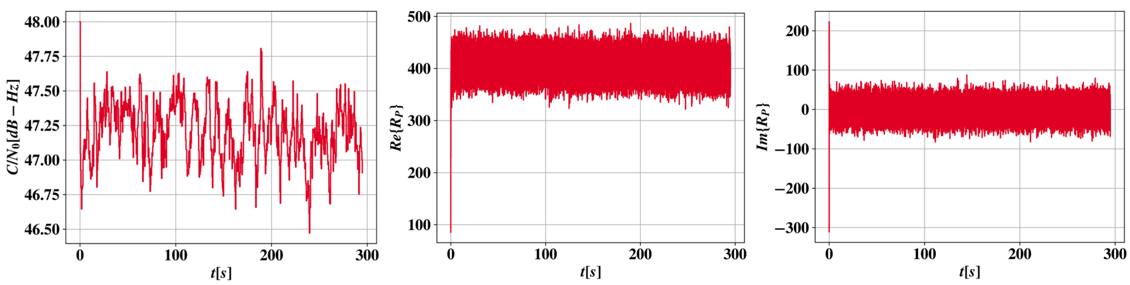

Figure 3.18: E33 - CN0, real, and imaginary part results variation.

As already mentioned, the rapid movement of LEO satellites across the sky leads to significant changes in signal strength over short times. The received power decreases as they move away from the receiver. This is illustrated in the plots of the real part variation, showing that, as the CN0 decreases (meaning low elevation angles and moving away), the received power also declines. This is the case of satellite L24, in Figure 3.17, serving as an excellent example of this behavior. In contrast, the real components for satellite E33, in Figure 3.18, remain relatively constant throughout the simulation. This occurs because, during the simulation period, E33 barely moves compared to L24, resulting in minimal variations in the received power.

As can be seen in Figure 3.19, satellite 24 starts the simulation with a Doppler shift close to zero, indicating the moment when it is near the receiver. As the simulation continues and just within 5 minutes, the satellite moves away from the receiver, resulting in a symmetric change on the Doppler shift values.

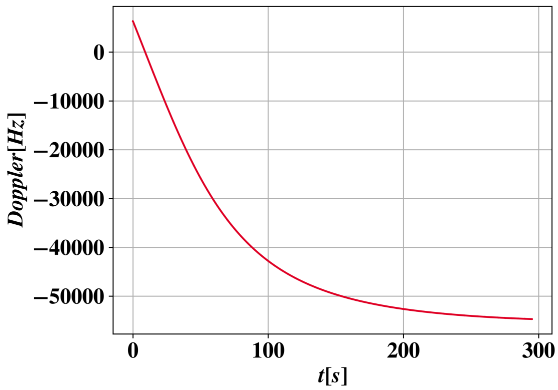

Figure 3.19: L24 - Doppler shift variation.

This behavior is expected, since the simulation begins when the satellite is closest to the receiver (doppler shift near zero), and the received power is also at its highest, as indicated by the real component of the signal.

In Figure 3.20 is presented the receiver's code delay accuracy for the different modulations considered. The code delay accuracy is defined here as the third order difference metric. Due to the satellite movement, and in order to assess the noise of the tracking, it is necessary to remove the dynamics. To achieve this, it is applied the third order difference method to fully assess the noise present in the code delay estimations, by removing the geometry contribution and doppler. This method, applied on four consecutive code observables, allows to determine instantaneously the code phase error, and assumes that the satellite's acceleration relative to the receiver is negligible compared to the code error. This is a useful method to filter the acceleration variations, specially when high dynamic conditions are present.

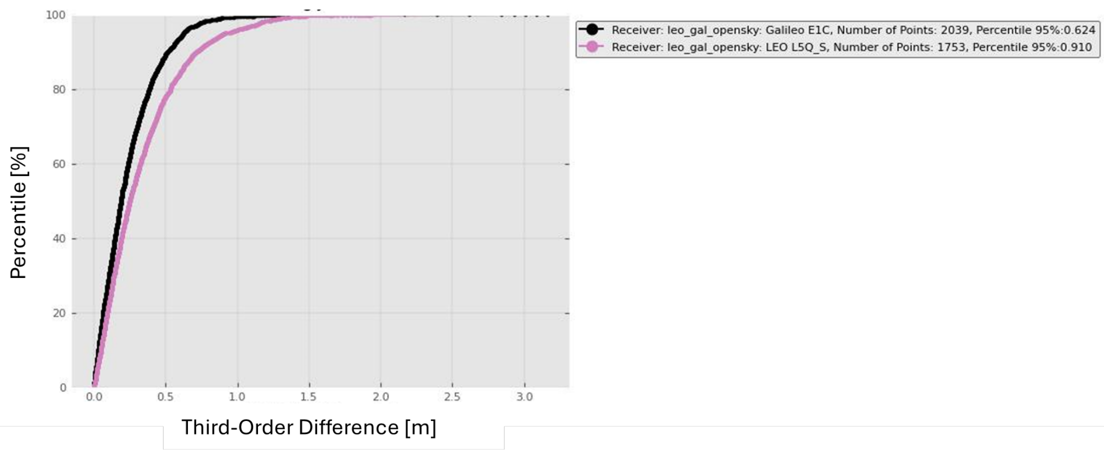

Figure 3.20: Code Tracking Jitter Percentile results.

This variable (code delay accuracy) provides the accuracy of the estimates and sheds some light on the expected values of the position solution. It is important to state that there is not a direct relation from this value to the position error, however, it is a good indicator of what can be achieved in the position solution and also to assess if the tracking loops are processing the signal as expected.

The X-axis may be interpreted as the magnitude of the jitter, the variation, or ranging error, in meters. Lower jitter values means the receiver is tracking the signal more smoothly. The Y-axis represents the percentage of the data points with the corresponding jitter values.

The 95th percentile is a standard measure often used to analyse performance data. At this value, Galileo E1C signal has a jitter of 0.624 meters, which is lower than the obtained value of 0.910 for LEO L5Q_S signal. Therefore, under most conditions, Galileo E1C signal offers better performance in terms of tracking stability when compared to LEO L5Q_S signal. This can be justified by the fast orbit of the LEO satellites, in which many points of the tracking are under noise conditions (low elevation). Since the MEO satellites have a "constant" carrier-to-noise ratio, all their estimates correspond to high values and do not decrease.

In Figure 3.21, it is possible to observe an increase of the code delay jitter for L24, represented by a larger "cloud" of points over time. This correlates with the observed CN0 plot for L24, in Figure 3.17, where the initial higher values of CN0 (representing the closest point to the receiver) correspond to a lower instantaneous range noise, as the estimates are more accurate during this period. The noise increases (represented by the larger "cloud" in Figure 3.21) as the CN0 values decrease.

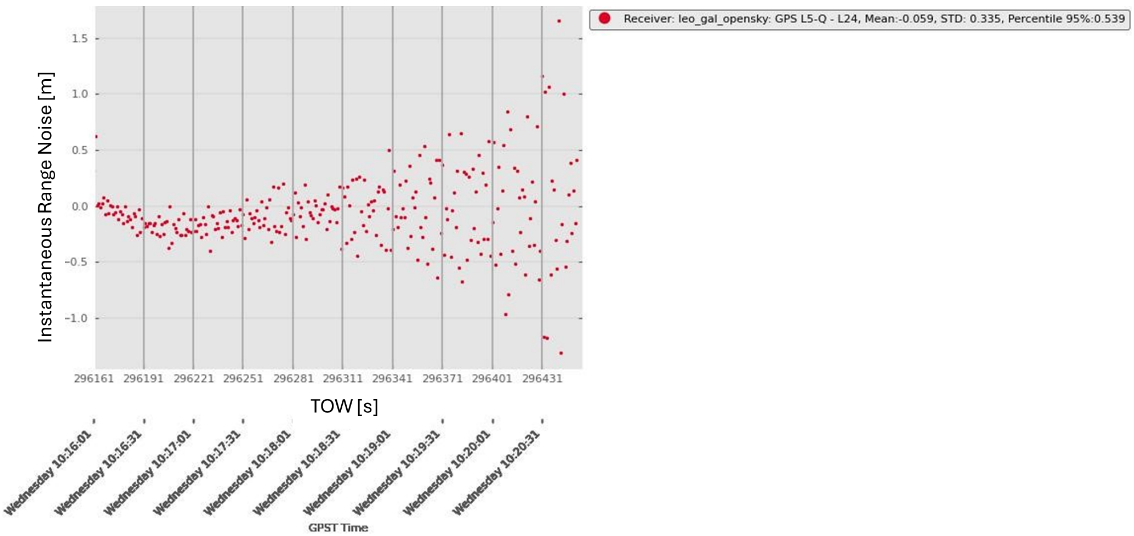

Figure 3.21: Code Tracking Jitter for L24.

In contrast, the instantaneous range noise for E33, observed in Figure 3.22, maintains a general constant value, which is also in accordance with its CN0 values, in Figure 3.18.

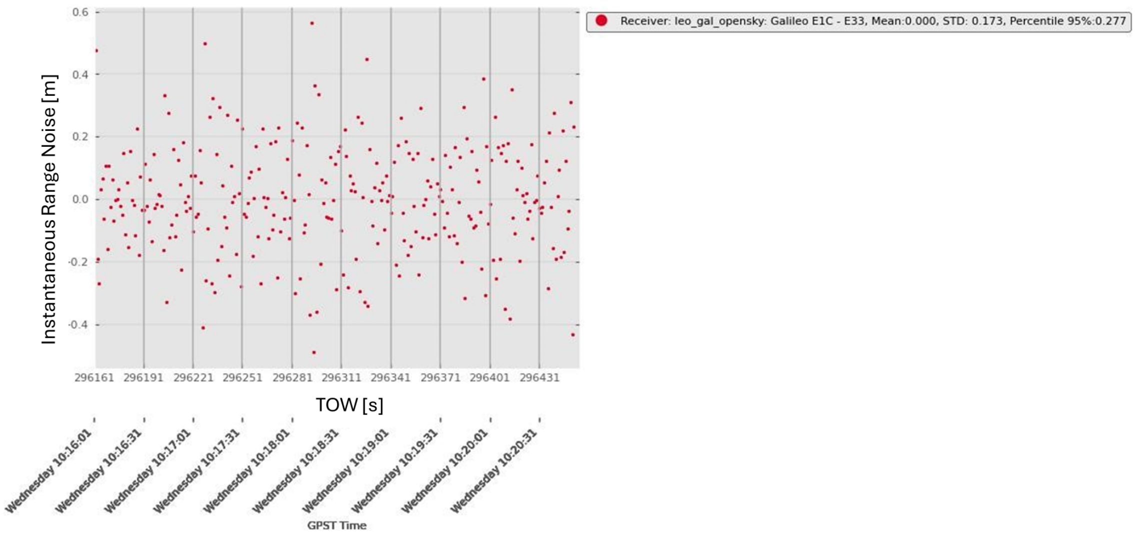

Figure 3.22: Code Tracking Jitter for E33.

Table 3.7 presents the code tracking jitter results for all satellites.

Table 3.7: Code Tracking Jitter results - Percentile 95%.

Code Tracking Jitter Percentile 95	E04	E10	E12	E19	E21	E26	E33	L04	L06	L08	L10	L11	L18	L24	L26	L27
E1C	0.539	0.696	0.469	0.432	0.615	0.577	0.277	nan	nan	nan	nan	nan	nan	nan	nan	nan
L5-Q	nan	nan	nan	nan	nan	nan	nan	0.971	0.677	0.649	0.690	0.979	0.436	0.539	1.071	0.715

It is possible to conclude that, despite LEO satellites having less than 15 minutes of visibility, only about half of that time provides accurate positioning estimates comparable to MEO satellites [63]. This highlights the challenges of LEO satellites, where only limited windows offer optimal signal quality.

It is important to note that, in open sky conditions, the LEO satellites contribution for a more accurate position are negligible due to the previous understanding. However, the aim of the LEO constellation, is for more demanding scenarios such as the ones to be analysed later: multipath and indoor conditions.

Figure 3.23 presents the overall doppler values for the different tracked satellites. Since Doppler effect is a critical factor in satellite communications, this graph is essential to understand the impact of the satellite motion on the signal tracking.

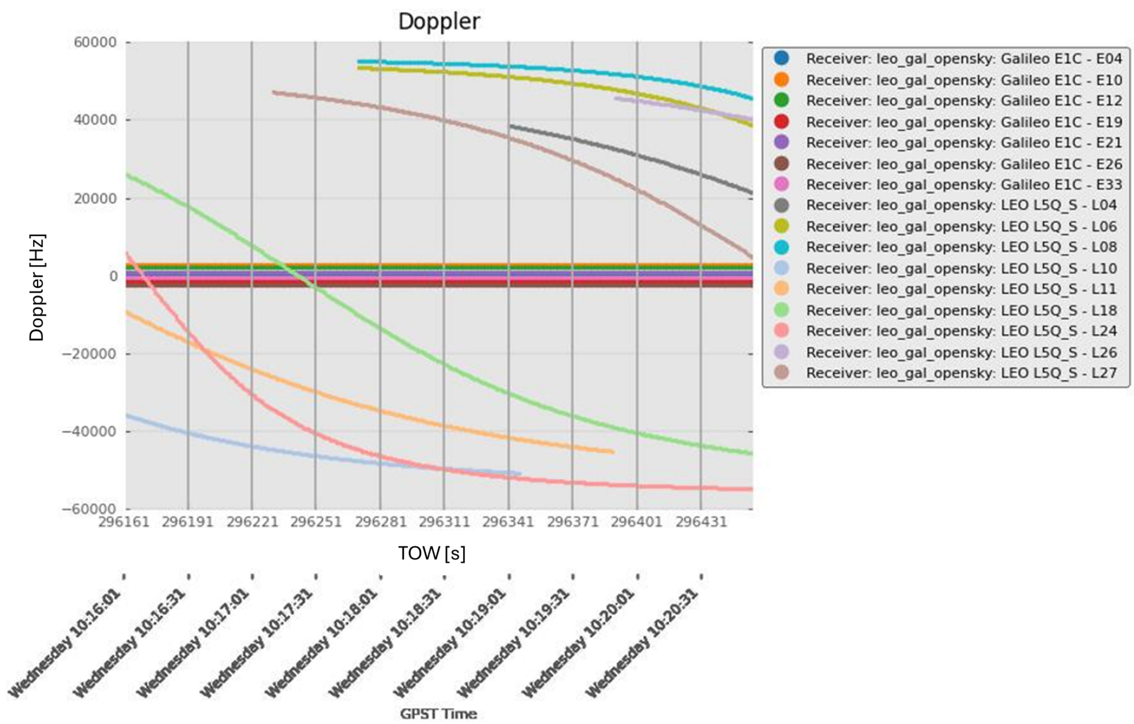

Figure 3.23: Doppler results.

LEO satellites show a much wider range of Doppler shifts, caused by the higher relative speed between those satellites and the receiver due to their lower orbital altitude, which results in rapid changes in signal frequency. In contrast, Galileo satellites almost appear static, and their Doppler shifts are clustered around -3kHz and 3kHz, which suggest a much lower relative motion between this satellites and the receiver.

Due to their high dynamic nature (only less than 15 minutes of visibility), and as previously analysed, the provided accuracy by LEO satellites, despite using a BPSK(10) modulation (which is theoretically more accurate than the CBOC(6,1,1/11) modulation of the Galileo satellites), is largely in line with the accuracy of Galileo's E1C signal. This means that the added value in terms of code delay accuracy is marginal. This is explained by the fact that approximately half of the visibility time is spent with low CN0 values (as the satellite enters and exits view) as previously analysed from the code accuracy study.

Figure 3.24 analyses the satellite availability.

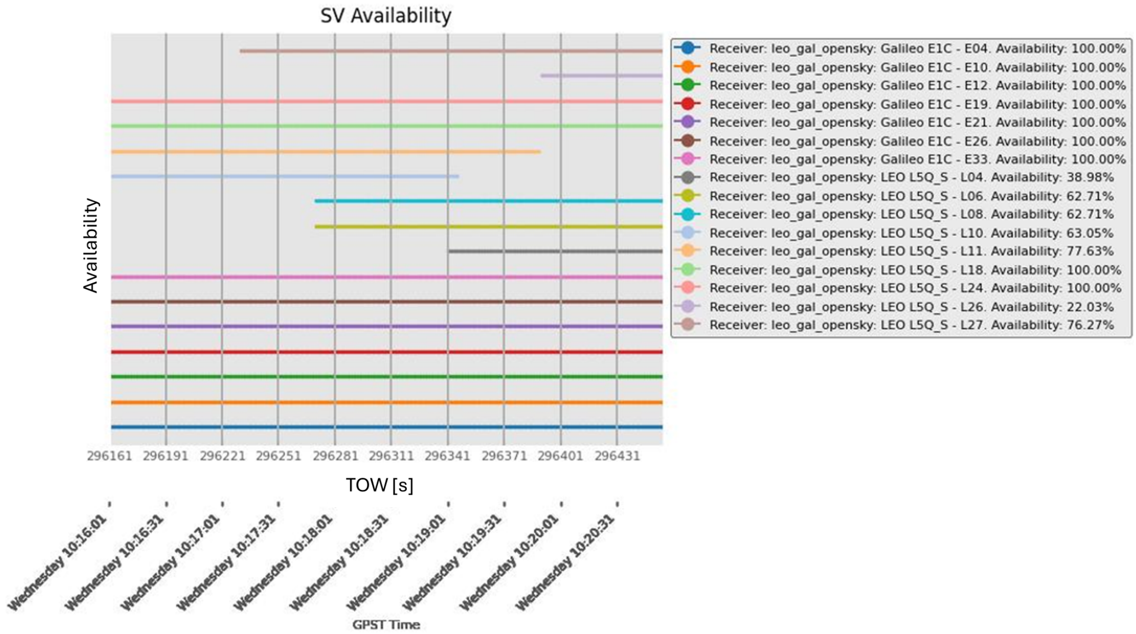

Figure 3.24: SV Availability.

This graph simply shows each satellite's availability over time. It reinforces the previous idea that LEO satellites are constantly entering and exiting view, which leads to lower accuracy. Only two LEO satellites show 100% of availability, L18 and L24, which are the best ones in terms of performance as also visible in the accuracy Table 3.7 (as these satellites are the ones with the lower code tracking jitter results, meaning higher accuracy).

It is important to highlight that, when new satellites enter the sky view in the middle of the simulation, their accuracy is generally weaker. However, when there is full visibility, it becomes possible to achieve the best accuracy for LEO satellites. In these cases, in approximately half of the time, we have high-quality BPSK(10) values, and during the other half (entering and exiting the sky view), worse values (as can be seen in Figure 3.21, where L24 has a good code tracking jitter for about half of the simulation time only). The average of these results aligns closely with the Galileo E1C signal at a CN0 of 42 dBHz (the code tracking jitter percentile has the same value for L24 and E04), as can be seen in Table 3.7. This means that, although the accuracy of LEO satellites may be affected at certain moments of the simulation, it is still comparable to the results obtained with Galileo, suggesting that the same accuracy can be achieved ultimately, even not being as reliable for a stand-alone system for continuous tracking.

3.2.3.1.2 PVT Performance Analysis

In this section it is analysed the Receiver Position Estimation Error over time for the base scenario (Galileo-only) and for GAL+LEO in open sky environments.

In order to analyse the accuracy of the PVT performance, the estimated position (in The Earth-Centered, Earth-Fixed (ECEF)) will be compared with the real position and its error will be analysed from the mean (bias) and standard deviation (stability) point of view.

In Figure 3.25 it is possible to assess the error in terms of the horizontal deviation.

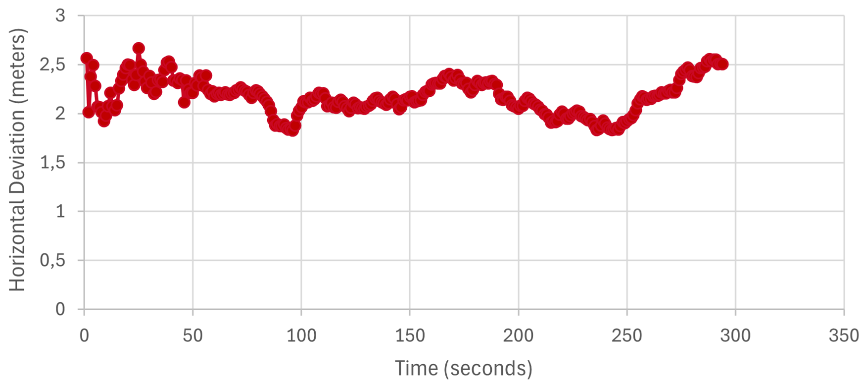

	X [m]	Y [m]	Z [m]
Mean Position - Full Simulation	1,96	-1,03	-0,18
STD of Position - Full Simulation	0,66	0,25	0,30
Mean Position - Last 50sec Simulation	2,02	-1,02	-0,20
STD of Position - Last 50sec Simulation	0,19	0,08	0,09

Figure 3.25: Horizontal Deviation and Mean and STD Deviation of Position Estimates (Full Simulation vs Last 50 seconds) for Galileo in Open Sky using Kalman Filter.

In the previous Figure it is shown the PVT error for the Galileo-only open sky scenario. As was previously seen in Figure 3.14(a), in the open sky scenario there are 7 Galileo satellites available, so it is expected to have a position with a high degree accuracy, and this is clearly seen in the values of Figure 3.25, especially if we consider the last 50 s of the simulation, in which the filter has already converged to the final values.

The standard deviation of the solution has a maximum value of 20 cm in the X-axis, with all of the other axis being below the 10 cm mark. When the full simulation is considered, these values are higher, but it is justified by the time that the Kalman filter takes to converge.

The performance is shown in Figure 3.26, but considering the full case of Galileo+LEO satellites.

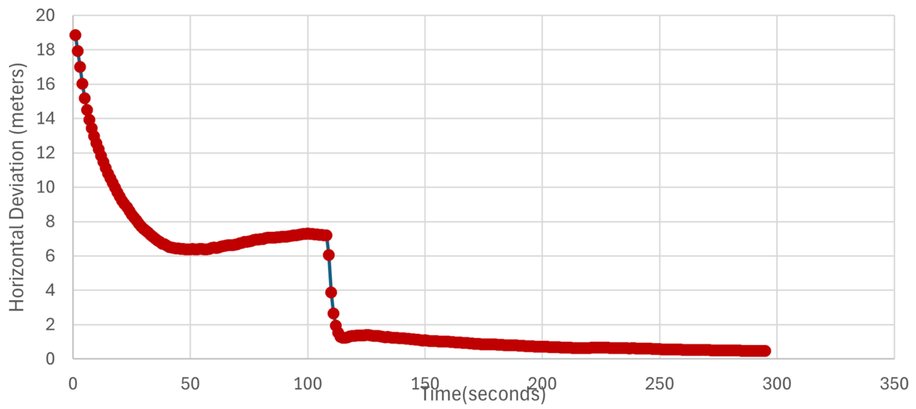

	X [m]	Y [m]	Z [m]
Mean Position - Full Simulation	0,58	-2,75	8,70
STD of Position - Full Simulation	2,17	3,86	9,14
Mean Position - Last 50sec Simulation	-0,52	0,08	0,66
STD of Position - Last 50sec Simulation	0,03	0,02	0,05

Figure 3.26: Horizontal Deviation and Mean and STD Deviation of Position Estimates (Full Simulation vs Last 50 seconds) for Galileo+LEO in Open Sky using Kalman Filter.

As can be seen in Figure 3.26, when the LEO constellation is also considered for the PVT computation in the open sky scenario, the position is more accurate, with reported standard deviation below 5 cm for the last 50 s of the simulation. This is a high improvement when compared with the Galileo-only scenario.

The same understanding is not true if the full simulation is considered. For this case, the Galileo-only scenario presents more accurate results (below 1 m) whereas the GAL+LEO has a STD value of approximately 2, 4 and 9 meters for the X, Y and Z axis, respectively. This behavior is clearly seen in the plots of Figure 3.26, in which the position takes a long time to converge to the right location. This behavior can be explained by the orbits of the LEO satellites, which take approximately 12 min for a full run across the sky. In contrast, for MEO satellites, this process takes several hours and during this time the number of visible satellites remains constant. Now, the number of available pseudoranges/satellites is always different along the simulation (as LEO satellites keep entering and exiting the solution) and the continuous input and ouput of new estimations on the PVT engine provokes the behavior seen in Figure 3.27.

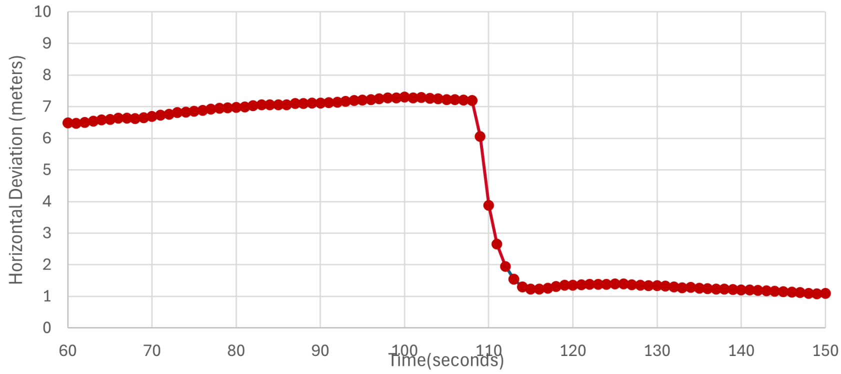

Figure 3.27: Detailed view on the PVT error time series for Galileo+LEO in Open Sky using Kalman Filter.

This is a very important point to take into account because it leads to the conclusion that PVT Engines should be reviewed when tracking MEO+LEO satellites. It is mandatory to improve this feature so it can be in the same order of performance as with only the MEO satellites.

In the next figure it is possible to find the same solution, but using a Least Squares instead of a Kalman Filter. As previously seen in subsection 2.2.2.1, Least Squares performs each estimation independently from the last one, which makes it invulnerable to the entering and exiting of satellites, as can be seen in Figure 3.28.

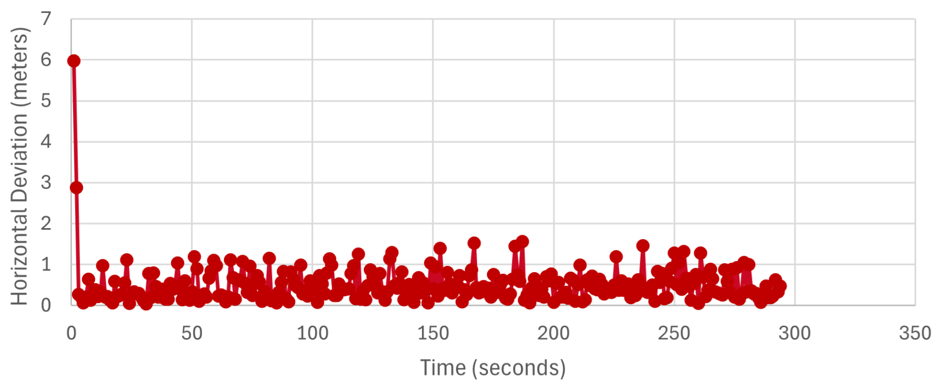

	X [m]	Y [m]	Z [m]
Mean Position - Full Simulation	0,01	-0,01	0,06
STD of Position - Full Simulation	0,91	0,92	1,60
Mean Position - Last 50sec Simulation	0,00	0,03	-0,07
STD of Position - Last 50sec Simulation	0,54	0,30	0,30

Figure 3.28: Horizontal Deviation and Mean and STD Deviation of Position Estimates (Full Simulation vs Last 50 seconds) for Galileo+LEO in Open Sky using LS.

By analyzing the results in Figure 3.28, the last 50 seconds of simulation and the full simulation reported results are very similar, which is expected due to the use of the LS solution. For the current technique, the entering and exiting of the satellites does not produce any issue regarding convergence of the solution, since for LS this is independent of previous measurements. This result also reinforces the fact that Kalman filter estimation should be assessed when implementing the use of LEO constellation for the final position estimation.

Galileo+LEO, Indoor, Kalman Filter

In the current subsection, results considering the indoor scenario are going to be presented. This scenario, as already stated, is the same scenario as previously analyzed, but only with two quadrants being considered (simulating, for example, a user next to a window).

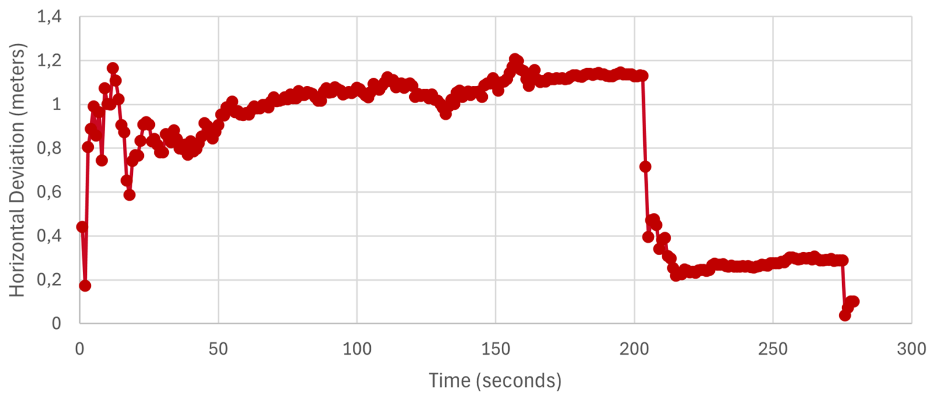

	X [m]	Y [m]	Z [m]
Mean Position - Full Simulation	0,81	0,07	0,13
STD of Position - Full Simulation	0,35	0,03	0,12
Mean Position - Last 50sec Simulation	0,26	0,05	-0,02
STD of Position - Last 50sec Simulation	0,06	0,01	0,01

Figure 3.29: Horizontal Deviation and Mean and STD Deviation of Position Estimates (Full Simulation vs Last 50 seconds) for Galileo+LEO in Indoor using Kalman Filter.

By analyzing the results in Figure 3.29, in indoor conditions, when both Galileo and LEO constellations are considered, it is possible to compute a solution for the full 5 minutes, being in line with the performance shown for the open sky scenario. This is a significant and relevant result, as it shows that not only is possible to have a positioning solution in indoor, but the performance achieved - due to the use of LEO satellites - is in line with the one shown for the open sky scenario (reference scenario), as can be seen in the tables of Figure 3.8.

Table 3.8: Positioning results for Galileo+LEO in Indoor scenario and Galileo+LEO in open sky scenario, respectively.

	Galileo+LEO Indoor			**Galileo+LEO Open sky**		
	X [m]	**Y [m]**	**Z [m]**	**X [m]**	**Y [m]**	**Z [m]**
Mean Position - Full Simulation	0,81	0,07	0,13	0,58	-2,75	8,70
STD of Position - Full Simulation	0,35	0,03	0,12	2,17	3,86	9,14
Mean Position - Last 50sec Simulation	0,26	0,05	-0,02	-0,52	0,08	0,66
STD of Position - Last 50sec Simulation	0,06	0,01	0,01	0,03	0,02	0,05

It is important to note that, with LEO satellites, when the filter is stable (represented by the last 50 s of the simulation) the accuracy increases significantly, since geometry plays a crucial role in accuracy. The LEO satellites not only provide more measurements, but also enhance the geometry of the constellation, which results in more precise positioning solutions.

Once again, it is important to notice the small discrepancies in the position, but as previously analysed, this happens due to the high number of satellites entering and exiting the position computation. However, for the current scenario, these are minimal, which is translated in the very high accuracy values reported previously.

3.2.3.2 Multipath Scenario

In this subsection it is analysed the tracking loops performance for Galileo signals and LEO L5Q_S in the multipath scenario, as previously defined in subsection 2.2.2.

3.2.3.3.1 Tracking Loop

In the current scenario, the key difference from the previous ones is the presence of signal impairments, which degrade the tracking performance. This can be observed in the tracking availability metrics shown in Table 3.9.

Table 3.9: SV Availability results without and with multipath, respectively.

Without Multipath				**With Multipath**			
SV	Availability	SV	Availability	SV	Availability	SV	Availability
E04:	100.00%	L04:	38.98%	E04:	-	L04:	38.98%
E10:	100.00%	L06:	62.71%	E10:	64.41%	L06:	62.71%
E12:	100.00%	L08:	62.71%	E12:	83.05%	L08:	62.71%
E19:	100.00%	L10:	63.05%	E19:	83.05%	L10:	-
E21:	100.00%	L11:	77.63%	E21:	83.05%	L11:	-
E26:	100.00%	L18:	100.00%	E26:	86.44%	L18:	-
E33:	100.00%	L24:	100.00%	E33:	86.44%	L24:	58.98%
		L26:	22.03%			L26:	22.03%
		L27:	76.27%			L27:	25.42%

As can be seen in Table 3.9, for most of the satellites, there is a clear degradation in availability, specially in the LEO signals. In the multipath scenario, three LEO satellites

(L10, L11, and L18) experienced a constant loss of lock and did not provide any estimates during the simulation. The same occurred for one Galileo MEO satellite, however, due to the high number of available Galileo MEO satellites, it should be possible to retrieve a position estimation without making use of the LEO measurements.

When examining the sky location of the loss of lock satellites (as shown in Figure 3.14), it is possible to see that a clear obstruction (a building, for example) is present between the 160º and 280º azimuth relative to the receiver. This is the main reason why no estimate could be retrieved from some satellites.

Finally, for the satellites that were able to provide measurements, the Galileo ones had an approximate 20% loss of availability and the LEO satellites L24 and L27 experienced availability degradation of approximately 41% and 51%, respectively.

As already mentioned and, despite losing several satellites, there are still six Galileo satellites remaining, which theoretically would be sufficient to provide a position by themselves without the need for LEO satellites. However, in urban scenarios such as city centers, the environment is constantly changing. From one moment to the next, an obstruction could block the azimuths where the Galileo satellites are located, making it impossible to retrieve a solution. For this reason, the addition of the LEO constellation is highly valuable, as it would allow to retrieve a position by using at least six satellites.

Due to the multipath effect, the carrier-to-noise ratio will be significantly affected when compared to the reference scenario, as shown in Figure 3.30.

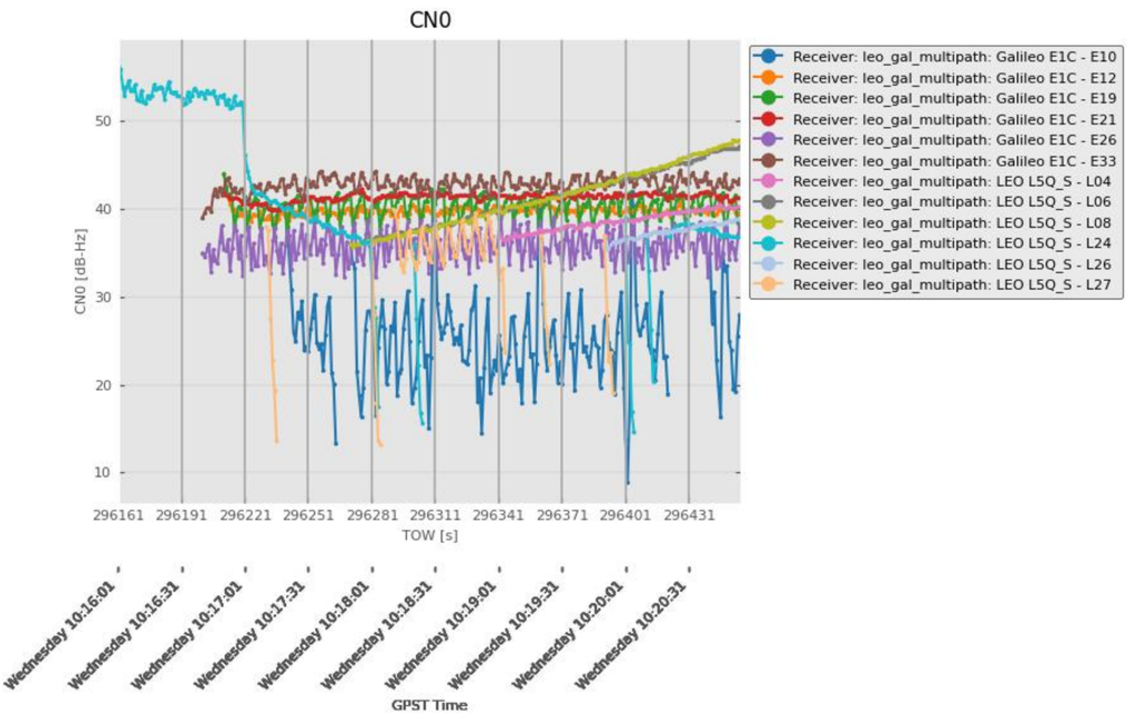

Figure 3.30: CN0 results in multipath scenario.

Table 3.10: CN0 - Mean values.

CN0 - Mean [db-Hz]	E04	E10	E12	E19	E21	E26	E33	L04	L06	L08	L10	L11	L18	L24	L26	L27
E1C	-	25.271	39.775	40.342	41.338	35.878	42.81	nan	nan	nan	nan	nan	nan	nan	nan	nan
L5-Q	nan	nan	nan	nan	nan	nan	nan	38.617	41.243	41.332	-	-	-	42.152	37.445	33.017

Figure 3.30 and Table 3.10 present the CN0 results in the multipath scenario, from which it is evident that there are significant fluctuations and drops for several satellites, unlike the previously analysed scenarios (like the ones presented previously in Table 3.6).

This fluctuations and variations are expected since it occurs due to the impact of the reflected signals, which are typical in urban environments, leading to overall degradation in the signal quality, as also assessed previously in the availability of the tracking in Table 3.9.

Even when the signal is tracked under multipath conditions, the obtained measurements are not reliable and highly noisy, leading to inaccuracies in the estimated position, as shown in Figure 3.31.

It is also important to note that, although L5Q_S signal uses BPSK(10) modulation, which is expected to be more resilient to multipath challenges, this satellites are in a lower altitude and with rapid movement, which makes them less susceptible to multipath (when in view), compared to MEO satellites. The frequent changes in position lead to more variations in the line-of-sight (LOS) paths between the satellite and the receiver, and if multipath exists, it will have a shorter impact when compared with MEO signals (the position of the satellite is "more constant"). So, given this circumstances, LEO satellites are shown to remain quite stable under this environments, even with these high fluctuations (comparing to MEO satellites), as can be seen in the Figure 3.31, depicting the code tracking jitter of the two different constellations.

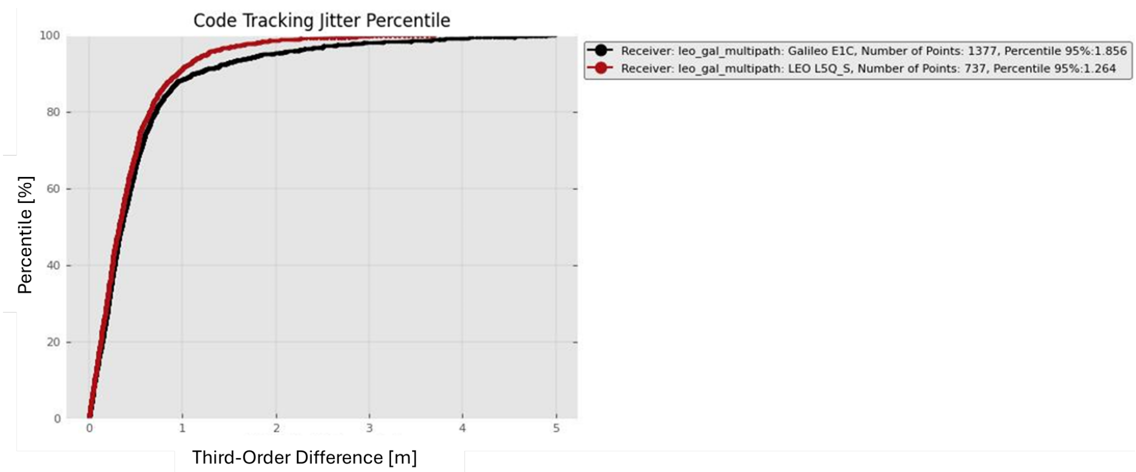

Figure 3.31: Code Tracking Jitter Percentile results in multipath scenario.

While in the open sky scenario the Galileo constellation satellites were more stable than the LEO ones, and this was reflected in the error regarding the 95th percentile of the code delay tracking error (Figure 3.20), in the current scenario the same is not true.

Due to the multipath impact in the signal, the Galileo constellation suffers variations in its power estimates and its performance is similiar with the one shown for LEO satellites. Because of this and the higher multipath rejection of BPSK(10), the LEO satellites' signals accuracy is more visible here, providing more accurate estimations with a 95th percentile code jitter of 1.3m versus the 1.9m of the E1C modulation.

These results align with the expected ones, given the nature of the modulation schemes used by both signals.

From the previous results it was shown that the main advantage of having LEO satellites added to the system is making it more robust by having a higher total number of satellites available to track and retrieve a position - rather than mitigating directly the multipath in the tracking loops or in the observation filter of the PVT engine. With the current strategy, many more measurements are available, leading to a more robust position estimation, which will be analyzed next.

3.2.3.3.2 Position Solution

In the next sections we present the results of the position for the multipath scenario. The position results will be organized according to the different constellations used, specifically the Galileo and the Galileo+LEO cases.

Galileo-only Solution

Figures 3.32 and 3.33 present the horizontal error of the position solution for the Galileo-only constellation, using Kalman Filter and Least Squares methods, respectively.

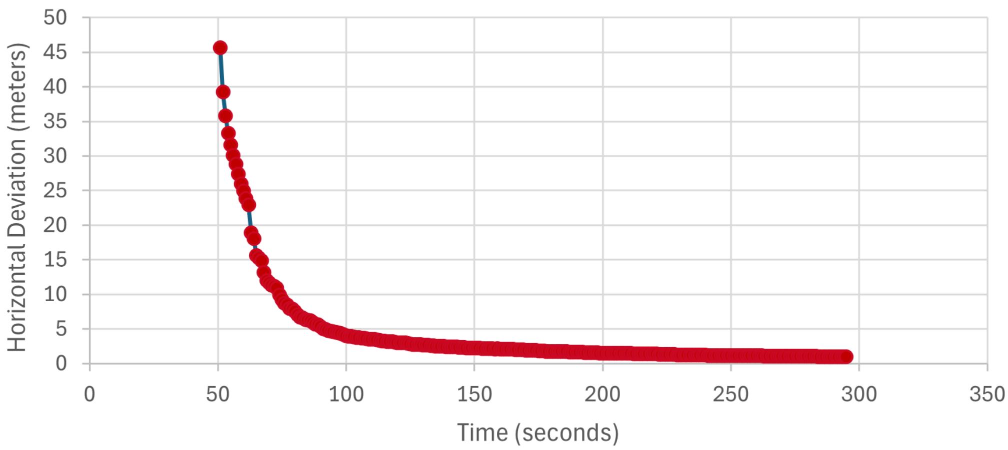

Figure 3.32: Position Horizontal Deviation for Galileo in Multipath scenario, using Kalman Filter.

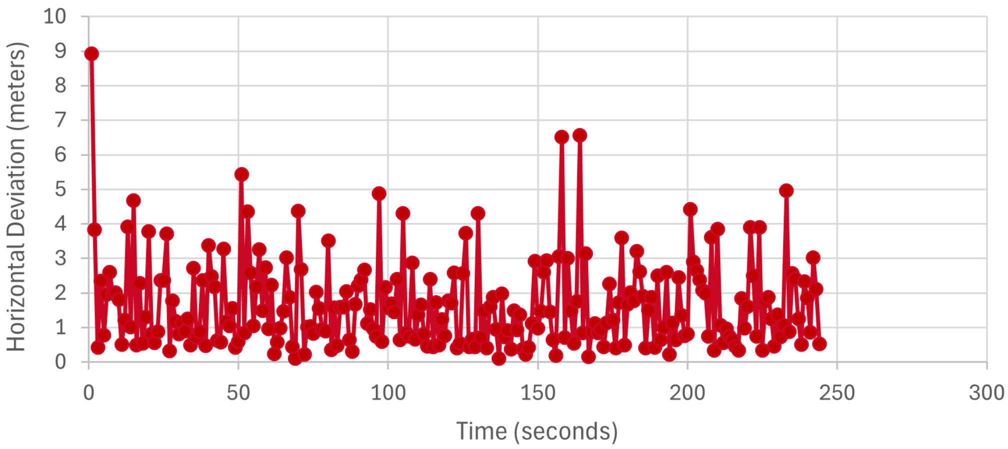

Figure 3.33: Position Horizontal Deviation for Galileo in Multipath scenario, using Least Squares.

From the previous Figures 3.32 and 3.33, it is possible to observe the difference between the Kalman Filter and the Least Squares estimator, as the convergence time of the first one is much longer than for the second one. Table 3.11 present the accuracy results for the current simulation.

Table 3.11: Mean and STD Deviation of Position Estimates (Full Simulation vs Last 50 seconds) for Galileo in Multipath scenario using Kalman Filter and Least Squares.

	Kalman Filter			Least Squares		
	X [m]	Y [m]	Z [m]	X [m]	Y [m]	Z [m]
Mean Position - Full Simulation	4,02	1,40	-2,98	0,44	0,06	-0,15
STD of Position - Full Simulation	6,42	2,44	5,11	3,36	1,21	2,31
Mean Position - Last 50sec Simulation	1,05	0,26	-0,60	0,26	0,04	-0,02
STD of Position - Last 50sec Simulation	0,05	0,02	0,04	1,92	0,69	1,13

For the current scenario, due to the already high availability of the Galileo satellites (with only one being blocked, E04, as shown in Table 3.9), the PVT engine is able to compute a solution despite the affected satellite. Because of this, the positioning errors are quite low if the last 50 seconds are taken for the Kalman solution (after filter convergence) and for the least squares (despite results being quite similar, for full and last 50 seconds, due to the nature of the solution, which is not smoothed and does not rely on previous estimates).

Since there is already a high number of available satellites and nearly two quadrants of the sky are blocked, the addition of LEO satellites in the current scenario is not expected to add benefit to the final solution. This is because it will not enhance the geometry, as the same area of the sky remains blocked and signal reflections occur independently of the distribution of satellite positions, nor the availability (given the high number of Galileo satellites under tracking).

Now that the Galileo-only test case has been analyzed, we can compare it with the Galileo+LEO solution to assess the added value of the newly designed constellation.

Galileo+LEO Solution

Figures 3.34, 3.35, and Table 3.12 present the horizontal error of the position solution and the mean and std deviation of Position Estimates for the Galileo+LEO constellation, using Kalman Filter and Least Squares methods, respectively.

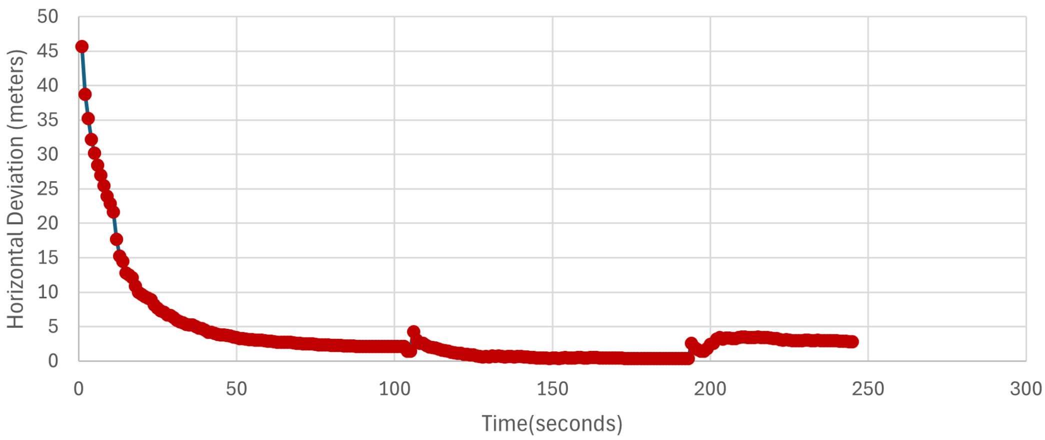

Figure 3.34: Position Horizontal Deviation for Galileo+LEO in Multipath scenario, using Kalman Filter.

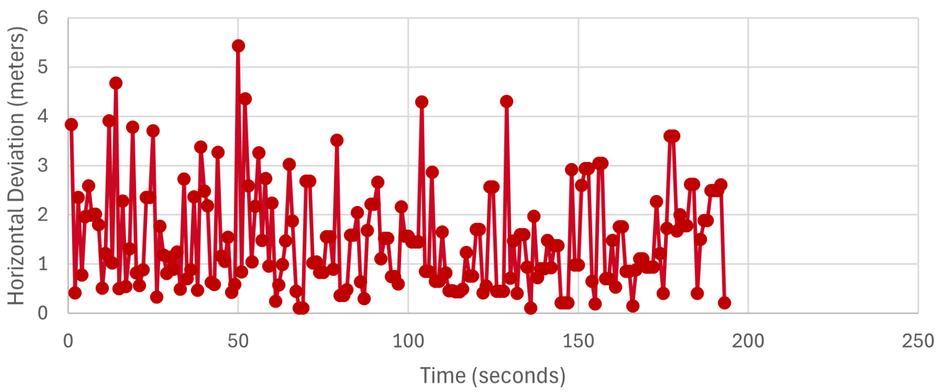

Figure 3.35: Position Horizontal Deviation for Galileo+LEO in Multipath scenario, using Least Squares.

Table 3.12: Mean and STD Deviation of Position Estimates (Full Simulation vs Last 50 seconds) for Galileo+LEO in Multipath scenario using Kalman Filter and Least Squares.

	Kalman Filter			**Least Squares**		
	X [m]	**Y [m]**	**Z [m]**	**X [m]**	**Y [m]**	**Z [m]**
Mean Position - Full Simulation	2,65	0,73	-1,66	0,42	0,07	-0,16
STD of Position - Full Simulation	6,54	2,64	5,41	3,25	1,16	2,21
Mean Position - Last 50sec Simulation	-2,29	-1,63	3,08	0,21	0,01	0,01
STD of Position - Last 50sec Simulation	1,08	0,33	0,78	1,56	0,56	0,81

When comparing the current results with the ones from the Galileo-only scenario (Table 3.11), they are overall quite similar for both solutions.

Due to the high availability of the Galileo satellites, the introduction of new satellites will only cause marginal improvements in positioning accuracy, as the initial solution (Galileo-only) is already performed using a large number of satellites, and the geometry does not improve with the LEO satellites (because, as already mentioned, reflections occur independently from the geometry).

This is evident in the results, where only slight improvements are observed with the addition of the LEO constellation. In fact, the accuracy slightly degrades when considering the Kalman filter solution.

Due to the high rate of satellites entering and exiting the PVT solution, it negatively impacts its accuracy. Therefore, special attention should be given to the PVT engine in order to deal and mitigate these fluctuations.

In contrast, the same conclusions are not drawn from the LS solutions, where the entry and exit of satellites have a minimal impact on the solution. When more LEO satellites are available (during the last 50 seconds of the simulation), the LS solution shows an overall improvement in accuracy, which is also in line with the previously analysed results in the code tracking loops, regarding the code accuracy, in Figure 3.31. Since there are more accurate measurements available, the PVT engine will prioritize these over the less accurate measurements from the E1C modulation, when computing the solution.

Even in scenarios where Galileo is able to provide a solution using only MEO satellites, the LEO constellation still has an added value, even being marginal.

It is important to emphasize, once again, that these urban scenarios are highly dynamic, and if a different azimuth range in the sky were blocked, the LEO satellites would not only provide the user a solution but also deliver a similar performance to the one encountered in the open sky scenario.

3.2.3.3 Main Conclusions

Based on the previous analysis of the positioning solutions through all the scenarios, the following key conclusions can be drawn:

- Performance with LEO Constellations: The PVT solution presents fluctuations (as depicted in Figure 3.27) when the LEO constellation measurements are added to the position solution. This is explained by the perturbations caused by the new satellite measurements entering and exiting the filtering solution. Additionally, contaminated environments, like in a multipath scenario, can lead to worse results.
- Kalman Filter Limitations: The Kalman filter generally shows improvement on the accuracy with the inclusion of LEO satellites in Open Sky conditions. However, it becomes less stable when high multipath interference is presented, due to the fast entering and exiting of new satellites, leading to jumps on the position estimates.
- Advantages of Least Squares: LS method shows a great robustness against fluctuations, caused by rapid changes in satellite visibility. The performance of the purposed system stays consistent in several scenarios, with a small impact when satellites entry or exit the visible area. This stability is crucial to obtain a reliable positioning, especially in challenging environments.
- Challenges in Multipath environments: Both Galileo and LEO constellations face significant challenges in this scenario. However, LEO satellites, by using the purposed BPSK(10) modulation, show a good resistance to this effects. Multipath becomes an important factor that affects positioning accuracy, which shows the need to implement effective multipath mitigation strategies in the future GNSS.
- Adaptation of PVT Engines: The analyzed results show the importance of adapting and improving PVT engines for PNT applications, in order to address the challenges caused by LEO constellations, challenging environments and its complexities. For this, special attention and fine tune tests need to be performed, in order to be able to deal with new circumstances that the innovative LEO constellations bring.
- Overall Performance Results: The combination of Galileo and LEO constellations generally shows improvement on the system robustness and coverage. However, the dynamic nature of LEO satellites requires careful consideration, design and development of PVT algorithms, capable of dealing with the introduced complexity.

Chapter 4

Conclusion and Future work

4.1 Conclusions

In the previous sections, a LEO constellation for PNT was designed, with an initial parameters proposal for the constellation, from an orbital (number and orbits of the constellation) and a signal (modulation, center frequency, power, among others) point of view. With the proposed designed system, and running signals mimicking this same system, it was possible to draw meaningful conclusions regarding the added value of the proposed constellation.

From a receiver processing perspective, the designed signals proved to add value to the considered scenarios. In the reference scenario, open sky, the inclusion of the LEO satellites was able to provide more accurate results than the one with only Galileo. During the analysis of this scenario, it was also noticed that the Kalman filter solution suffers from the constant inclusion of new measurements, and this should be a point to be further addressed when designing receivers able to cope with such constellations.

It was also visible that the higher dynamics of the LEO satellites when compared with the MEO ones, bring an added challenge for the tracking engine, which needs to be adapted in order to cope with the new signals. This point was successfully performed in the current study, with fine tuning and the best configurations found for the problem at hand.

When analyzing the more demanding scenarios, for the indoor case, the inclusion of the LEO satellites was fundamental and necessary in order to have a position. Without these satellites, a solution was not possible to be provided, due to the low number of available Galileo satellites. Since indoor scenarios have always been one of the weaker points of the GNSS solution, it is possible to conclude that, with the inclusion of LEO satellites, an accurate solution can be available just by relying on the Galileo constellation, considering MEO+LEO.

In the multipath scenario, the added value and benefits of the LEO constellation could not be fully assessed, as is the case for the indoor one, because the PVT engine was able to remove the erroneous measurements only with the Galileo MEO constellation, being able to provide an accurate and reliable positioning without the need for LEO satellites. In these circumstances, the inclusion of more satellites will not provide a higher robustness and the added accuracy will be marginal, as seen in the results. However, if a more demanding multipath scenario was considered, the scenario would be closer to the indoor one, and the inclusion of the LEO satellites would prove to be fundamental in order to gather a position.

Therefore, LEO satellites effectively complement the Galileo system, enabling it to function as a stand-alone solution to achieve high levels of precision. This is particularly valuable in environments where traditional GNSS signals would struggle due to limited satellite availability.

4.2 Future Work

In the current work, several points for future work improvement were identified in order to make the LEO constellation suitable and capable of providing higher robustness and accuracy in the GNSS positioning, such as:

- The design of the link budget of the constellation should be carefully addressed. This is essential to ensure that LEO signals will provide a higher robustness to the position solution. Key factors include defining the central frequency to avoid interference with existing signals, determining the signal power, and choosing the right modulation scheme, since the accuracy of new signals is linked to these design choices. Additionally, the orbit and number of satellites to be deployed must be optimal to ensure a meaningful sky plot with sufficient LEO satellites, enabling Galileo to function as a single constellation solution in most scenarios. This Thesis presents an initial proposal, so further work should be performed on all of these aspects to fully define the system.

- It was assessed that the PVT engine, when computing the Kalman filter solution, faces some fluctuations in its position estimate due to the constant entering and exiting of new LEO satellites. A robust design should be implemented into the PVT engine to accommodate this new understanding. Additionally, fine-tuning should be performed in terms of the smoothing time and new adaptations in the Kalman filter, to better adapt the new signals coming from the LEO satellites in the final positioning solution.

- To draw more realistic conclusions regarding the added value of a LEO constellation, a diverse array of different multipath, indoor, and multi-dynamic user scenarios should be considered, in order to have a full overview of the benefits and downsides of the new constellation. This way, work can be performed to improve the solution by using the proposed LEO constellation.

Bibliography

[1] C. Pinell et al. "Receiver architectures for positioning with low earth orbit satellite signals: a survey". In: *EURASIP Journal on Advances in Signal Processing* 2023 (2023-06). DOI: 10.1186/s13634-023-01022-1 (cit. on pp. 1, 24, 25).

[2] *What are LEO Satellites and why are they good for PNT?* Safran. URL: https://safran-navigation-timing.com/what-are-leo-satellites-and-why-are-they-good-for-pnt/ (visited on 2024-01-18) (cit. on pp. 1, 24).

[3] *What is GNSS?* European Union Agency for the Space Programme, 2023-12. URL: https://www.euspa.europa.eu/european-space/eu-space-programme/what-gnss (visited on 2023-12-20) (cit. on p. 5).

[4] *GNSS constellations: differences, what have in common and vulnerabilities?* LinkedIn. URL: https://www.linkedin.com/pulse/gnss-constellations-differences-what-have-common-marco-romani (visited on 2024-01-24) (cit. on p. 5).

[5] G. Falco, A. Favenza, and M. Nicola. "Data decoding of the first Galileo IOV PFM satellite and joint GPS+Galileo positions". In: *2012 International Conference on Localization and GNSS*. 2012, pp. 1–7. DOI: 10.1109/ICL-GNSS.2012.6253130 (cit. on p. 5).

[6] *1.2 GLOBAL NAVIGATION SATELLITE SYSTEM (GNSS)*. Vectornav. URL: https://www.vectornav.com/resources/inertial-navigation-primer/theory-of-operation/theory-gnss (visited on 2023-12-25) (cit. on p. 5).

[7] A. Kornhauser. *Global Navigation Satellite System (GNSS)*. Tech. rep. 2006 (cit. on p. 6).

[8] O. M. Peter J.G. Teunissen. *Springer Handbook of Global Navigation Satellite Systems*. 1st ed. Massachusetts: Springer Cham, 2021. DOI: https://doi.org/10.1007/978-3-319-42928-1 (cit. on pp. 6, 7, 9–11, 14, 16, 19–21, 39, 42).

[9] *Galileo Services*. European Space Agency. URL: https://gssc.esa.int/navipedia/index.php/Galileo_Services (visited on 2023-12-25) (cit. on p. 6).

[10] *GNSS Spectrum Allocation*. EUROCONTROL. URL: https://pbnportal.eu/epbn/main/Overview-of-PBN/PBN-Concept---Unpacked/PBN-Infrastructure/Space-based/GNSS-Spectrum-Allocation.html (visited on 2024-01-03) (cit. on p. 6).

[11] "European GNSS (Galileo) - Open Service - Signal-In-Space Interface Control Document". In: (2021) (cit. on pp. 6, 8, 9, 29, 38, 40).

[12] L. Ortega Espluga. "Signal optimization for Galileo evolution". Theses. Institut National Polytechnique de Toulouse - INPT, 2019-11. URL: https://theses.hal.science/tel-04169759 (cit. on pp. 7–9).

[13] M. Foucras. "Performance Analysis of the Modernized GNSS Signal Acquisition". Theses. Institut National Polytechnique de Toulouse - INPT, 2015-02. URL: https://theses.hal.science/tel-04229743 (cit. on pp. 7, 11, 17).

[14] R. Khan et al. "Acquisition Strategies of GNSS Receiver". English. In: *Proceedings of 2011 International Conference on Computer Networks and Information Technology (ICCNIT)*. IEEE International Conference on Computer Networks and Information Technology, ICCNIT 2011 ; Conference date: 11-07-2011 Through 13-07-2011. Institute of Electrical and Electronics Engineers Inc., 2011, pp. 119–124. ISBN: 978-1-61284-940-9. DOI: 10.1109/ICCNIT.2011.6020917 (cit. on pp. 7, 19–22).

[15] P. Das et al. "Performance Limits of GNSS Code-Based Precise Positioning: GPS, Galileo & Meta-Signals". In: *Sensors* 20.8 (2020). ISSN: 1424-8220. DOI: 10.3390/s20082196. URL: https://www.mdpi.com/1424-8220/20/8/2196 (cit. on p. 7).

[16] *GNSS signal modelling considering channel impairments and spoofing interferences*. Wasy Research. URL: https://www.wasyresearch.com/gnss-signal-modelling-considering-channel-impairments-and-spoofing-interferences/ (visited on 2024-01-16) (cit. on p. 8).

[17] *Technical details of current Galileo signal*. European Space Agency. URL: https://www.esa.int/Applications/Navigation/Technical_details_of_current_Galileo_signal (visited on 2024-01-26) (cit. on p. 8).

[18] M. Foucras et al. "A Novel Computationally Efficient Galileo E1 OS Acquisition Method for GNSS Software Receiver". In: vol. 1. 2012-09 (cit. on p. 8).

[19] *GNSS Modulation Schemes*. European Space Agency. URL: https://gssc.esa.int/navipedia/index.php/GNSS_Modulation_Schemes (visited on 2024-01-11) (cit. on p. 9).

[20] *DS-SS (Direct-sequence spread spectrum)*. Telecom Trainer. URL: https://www.telecomtrainer.com/ds-ss-direct-sequence-spread-spectrum/ (visited on 2024-01-11) (cit. on p. 10).

[21] *BPSK – Binary Phase Shift Keying*. GeeksforGeeks. URL: https://www.geeksforgeeks.org/bpsk-binary-phase-shift-keying/ (visited on 2024-01-14) (cit. on p. 10).

[22] R. C. Pedrós. *Galileo Signal Generation - Simulation Analysis*. Tech. rep. 2009. URL: https://upcommons.upc.edu/bitstream/handle/2099.1/7615/Project%20Galileo.pdf (cit. on pp. 10, 11).

[23] *Binary Offset Carrier (BOC)*. European Space Agency. URL: https://gssc.esa.int/navipedia/index.php/Binary_Offset_Carrier_(BOC) (visited on 2024-01-11) (cit. on pp. 10, 11).

[24] A. Grenier et al. "A Survey on Low-Power GNSS". In: *IEEE Communications Surveys & Tutorials* PP (2023-04). DOI: 10.1109/COMST.2023.3265841 (cit. on p. 11).

[25] *Galileo Navigation Message*. European Space Agency. URL: https://gssc.esa.int/navipedia/index.php?title=Galileo_Navigation_Message (visited on 2024-01-06) (cit. on p. 12).

[26] *Keplerian Paramters*. Galileo GNSS. URL: https://galileognss.eu/ephemeris-keplerian-parameters/ (visited on 2024-01-08) (cit. on pp. 12, 13).

[27] J. Subirana et al. *GNSS Data Processing, Vol. I: Fundamentals and Algorithms*. ESA TM vol. 1. ESA Communications, 2013. ISBN: 9789292218867. URL: https://books.google.es/books?id=RO8xngEACAAJ (cit. on pp. 12, 13, 15).

[28] *Galileo satellites*. European Space Agency. URL: https://www.esa.int/Applications/Navigation/Galileo/Galileo_satellites (visited on 2024-01-16) (cit. on p. 13).

[29] R. Zhang et al. "Performance of Galileo: Global coverage, precise orbit determination, and precise positioning". In: *Advances in Space Research* 64.2 (2019), pp. 299–313. ISSN: 0273-1177. DOI: https://doi.org/10.1016/j.asr.2019.03.042. URL: https://www.sciencedirect.com/science/article/pii/S027311771930239X (cit. on p. 13).

[30] *Galileo Space Segment*. European Space Agency. URL: https://gssc.esa.int/navipedia/index.php/Galileo_Space_Segment (visited on 2024-01-16) (cit. on p. 13).

[31] *GNSS Basic Observables*. European Space Agency. URL: https://gssc.esa.int/navipedia/index.php/GNSS_Basic_Observables (visited on 2024-01-14) (cit. on p. 14).

[32] *Baseband Processing*. European Space Agency. URL: https://gssc.esa.int/navipedia/index.php?title=Baseband_Processing (visited on 2024-01-14) (cit. on p. 16).

[33] *Generic Receiver Description*. European Space Agency, 2011. URL: https://gssc.esa.int/navipedia/index.php/Generic_Receiver_Description (visited on 2024-01-16) (cit. on p. 17).

[34] *Correlators*. European Space Agency, 2014. URL: https://gssc.esa.int/navipedia/index.php/Correlators (visited on 2024-01-18) (cit. on pp. 18, 19).

[35] F. van Diggelen. *GPS: An Introduction to Satellite Navigation*. Youtube. 2014. URL: https://www.youtube.com/watch?v=sou7aab8w4o&list=PLGvhNIiu1ubyEOJga50LJMzVXtbUq6CPo&index=36 (visited on 2024-01-11) (cit. on p. 18).

[36] P. A. M. Boto. "Analysis and Development of Algorithms for Fast Acquisition of Modern GNSS Signals". PhD thesis. 2014-12 (cit. on p. 20).

[37] *Tracking Loops*. European Space Agency. URL: https://gssc.esa.int/navipedia/index.php/Tracking_Loops (visited on 2024-01-17) (cit. on pp. 20, 21).

[38] *GNSS Receivers General Introduction*. European Space Agency. URL: https://gssc.esa.int/navipedia/index.php/GNSS_Receivers_General_Introduction (visited on 2024-01-17) (cit. on p. 22).

[39] T. R. Peres. "Multipath Mitigation Techniques Suitable For Low Cost GNSS Receivers". In: 2008. URL: https://api.semanticscholar.org/CorpusID:264693604 (cit. on p. 22).

[40] N. Rahemi and M. Mosavi. "Positioning accuracy improvement in high-speed GPS receivers using sequential extended Kalman filter". In: *IET Signal Processing* 15 (2021-04). DOI: 10.1049/sil2.12027 (cit. on p. 23).

[41] R. M. Ferre et al. "Is LEO-Based Positioning with Mega-Constellations the Answer for Future Equal Access Localization?" In: *IEEE Communications Magazine* 60.6 (2022), pp. 40–46. DOI: 10.1109/MCOM.001.2100841 (cit. on p. 24).

[42] F. S. Prol et al. "Position, Navigation, and Timing (PNT) Through Low Earth Orbit (LEO) Satellites: A Survey on Current Status, Challenges, and Opportunities". In: *IEEE Access* 10 (2022), pp. 83971–84002. DOI: 10.1109/ACCESS.2022.3194050 (cit. on pp. 24–26).

[43] M. Su et al. "BeiDou Augmented Navigation from Low Earth Orbit Satellites". In: *Sensors* 19.1 (2019). ISSN: 1424-8220. DOI: 10.3390/s19010198. URL: https://www.mdpi.com/1424-8220/19/1/198 (cit. on pp. 24, 25).

[44] L. Cheng et al. "Structure and Performance Analysis of Signal Acquisition and Doppler Tracking in LEO Augmented GNSS Receiver". In: *Sensors* 21.2 (2021). ISSN: 1424-8220. DOI: 10.3390/s21020525. URL: https://www.mdpi.com/1424-8220/21/2/525 (cit. on p. 25).

[45] *Large Constellations of Low-Altitude Satellites: A Primer*. Congressinal Budget Office. URL: https://www.cbo.gov/publication/59175#_idTextAnchor047 (visited on 2024-01-25) (cit. on pp. 25, 26).

[46] A. Atayero, M. Luka, and A. Alatishe. "Satellite Link Design: A Tutorial". In: *International Journal of Electrical Computer Sciences* 11 (2011-08), pp. 1–6 (cit. on p. 27).

[47] F. Ma et al. "Hybrid constellation design using a genetic algorithm for a LEO-based navigation augmentation system". In: *GPS Solut.* 24.2 (2020). ISSN: 1080-5370. DOI: 10.1007/s10291-020-00977-0. URL: https://doi.org/10.1007/s10291-020-00977-0 (cit. on pp. 28, 29).

[48] C. J. R. Capela. "Protocol of communications for VORSat satellite". In: 2012. URL: https://api.semanticscholar.org/CorpusID:110594265 (visited on 2024-09-18) (cit. on p. 30).

[49] M. Imad et al. "Ionospheric Error Models for Satellite-Based Navigation—Paving the Road towards LEO-PNT Solutions". In: *Computers* 13.1 (2024). ISSN: 2073-431X. DOI: 10.3390/computers13010004. URL: https://www.mdpi.com/2073-431X/13/1/4 (cit. on p. 30).

[50] J. Kokkoniemi et al. "Channel Modeling and Performance Analysis of Airplane-Satellite Terahertz Band Communications". In: *IEEE Transactions on Vehicular Technology* PP (2021-02), pp. 1–1. DOI: 10.1109/TVT.2021.3058581 (cit. on p. 30).

[51] K. Wang, S. Zhang, and J. Wang. "Feasibility of using an S-band GNSS carrier by comparing with L and C bands". In: *Advances in Space Research* 66.9 (2020), pp. 2232–2244. ISSN: 0273-1177. DOI: https://doi.org/10.1016/j.asr.2020.07.029. URL: https://www.sciencedirect.com/science/article/pii/S0273117720305366 (cit. on pp. 30, 31).

[52] J.-A. Avila-Rodriguez et al. "A vision on new frequencies, signals and concepts for future GNSS systems". In: *Proceedings of the 20th International Technical Meeting of the Satellite Division of the Institute of Navigation, Fort Worth, TX, USA* (2007-01) (cit. on pp. 30, 31).

[53] *ESA encourages S-band applications with NovaSAR-1 Announcement of Opportunity*. European Union Agency for the Space Programme, 2024-01. URL: https://earth.esa.int/eogateway/news/esa-encourages-s-band-applications-with-novasar-1-announcement-of-opportunity (visited on 2024-04-15) (cit. on p. 31).

[54] H. Liu. "BPSK/BOC Modulation Signal System for GPS Satellite Navigation Signals". In: *Journal of Physics: Conference Series* 2384 (2022-12), p. 012023. DOI: 10.1088/1742-6596/2384/1/012023 (cit. on p. 31).

[55] *NORAD GP Element Sets Current Data*. CelesTrak. URL: https://celestrak.org/NORAD/elements/ (visited on 2024-07-15) (cit. on pp. 32, 35).

[56] B. Kujur, S. Khanafseh, and B. Pervan. "Experimental Validation of Optimal INS Monitor against GNSS Spoofer Tracking Error Detection". In: 2023-04, pp. 592–596. DOI: 10.1109/PLANS53410.2023.10140096 (cit. on p. 34).

[57] B. Krach, A. Lehner, and A. Steingass. "Technical Note on the Implementation of the Land Mobile Satellite Channel Model - Software Usage". In: (2005-11) (cit. on p. 38).

[58] S. E. Defense. *Skydel - User Manual*. Tech. rep. 2024 (cit. on p. 41).

[59] V. Janssen. "Understanding the RINEX format for GNSS data transfer and storage". In: 19 (2023-11), pp. 20–27 (cit. on p. 41).

[60] *XRC*. GMV Innovating Solutions. URL: https://www.gmv.com/en-pt/products/space/xrc#key-features-39746 (visited on 2024-07-29) (cit. on p. 41).

[61] J. Pei and Z.-q. Hu. "Third-order carrier PLL design and analysis for high dynamic performance". In: *IET International Communication Conference on Wireless Mobile and Computing (CCWMC 2011)*. 2011, pp. 76–79. DOI: 10.1049/cp.2011.0850 (cit. on pp. 43, 44).

[62] J. Vilà-Valls et al. "Are PLLs dead? A tutorial on kalman filter-based techniques for digital carrier synchronization". In: *IEEE Aerospace and Electronic Systems Magazine* 32 (2017-07), pp. 28–45. DOI: 10.1109/MAES.2017.150260 (cit. on p. 44).

[63] "Satellite Visibility Prediction". In: *Doppler Applications in LEO Satellite Communication Systems: CD-Rom Included*. Boston, MA: Springer US, 2002, pp. 53–66. ISBN: 978-0-306-47546-7. DOI: 10.1007/0-306-47546-4_4. URL: https://doi.org/10.1007/0-306-47546-4_4 (cit. on p. 50).

2024 Dissertation Report

Beatriz

NOVA SCHOOL OF SCIENCE & TECHNOLOGY